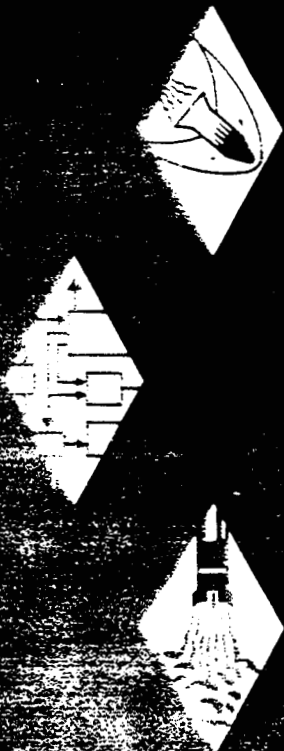


AEROSPACE RESEARCH • AERODYNAMICS • PROPULSION • STRUCTURAL DYNAMICS • ELECTRONIC SYSTEMS AND INSTRUMENTS • COMPUTER MODULES



RESEARCH
ENGINEERING
PRODUCTION

EXPERIMENTAL DETERMINATION OF HEAT
TRANSFER DUE TO HYDROGEN COMBUSTION
IN BASE FLOW REGION

TECHNICAL REPORT NO. 625

FINAL REPORT

N67-31186
(ACCESSION NUMBER)
62
(PAGES)
CR-85819
(NASA CR OR TMX OR AD NUMBER)

(THRU)
0
(CODE)
33
(CATEGORY)

REPRODUCED BY
U.S. DEPARTMENT OF COMMERCE
NATIONAL TECHNICAL
INFORMATION SERVICE
SPRINGFIELD, VA 22161

GENERAL APPLIED SCIENCE LABORATORIES, INC.
MERRICK and STEWART AVENUES, WESTBURY, L.I., N.Y. • (516) ED 3-6960

57/43769

GASL Job #8006.
Contract No. NAS8-2686

Page i
Copy (27) of (3)

EXPERIMENTAL DETERMINATION OF HEAT TRANSFER DUE
TO HYDROGEN COMBUSTION IN A BASE FLOW REGION

TECHNICAL REPORT NO. 625

FINAL REPORT

by

C. Economos

Prepared for

National Aeronautics and Space Administration
Huntsville, Alabama

Prepared by

General Applied Science Laboratories, Inc.
Merrick and Stewart Aves.
Westbury, L.I., N.Y.

Approved by:

M. Mandel for

A. Ferri
President

October, 1966

EXPERIMENTAL DETERMINATION OF HEAT
TRANSFER DUE TO HYDROGEN COMBUSTION
IN A BASE FLOW REGION

TECHNICAL REPORT No. 625

FINAL REPORT

October 1966

SUMMARY

Measurements of heat transfer, pressure, and recovery temperature at the blunt base of a circular cylinder with and without combustion of hydrogen in the recirculation zone have been obtained.

The tests were conducted at Mach numbers 0.23 and 3, and the boundary layer at the shoulder appeared to be turbulent. The hydrogen was introduced by tangential injection upstream of the shoulder. Combustion was induced at Mach 3 by autoignition utilizing sufficiently high flow stagnation temperatures and at Mach .23 by means of an electric spark. The extent to which the hydrogen was entrained in the recirculation zone was established quantitatively by fuel concentration measurements in the vicinity of the base. It was found that the effect of combustion on the base properties could be correlated in terms of this fuel concentration. Utilizing this parameter, an empirical procedure for estimating the recovery temperature and increase in heating rates associated with combustion has been deduced and is described herein.

TABLE OF CONTENTS

<u>Section</u>	<u>Title</u>	<u>Page No.</u>
	Summary	ii
	List of Figures	iv
	List of Symbols	vi
I	Introduction	1
II	Description of Experimental Equipment	3
III	Presentation and Discussion of Results	9
IV	Conclusions	22
V	References	23
	Table I and II	26
	Figures	27

LIST OF FIGURES

<u>Figure No.</u>	<u>Title</u>	<u>Page No.</u>
1	Schematic of Model and Nozzle Configuration	27
2	Location of Instrumentation on Base Model	28
3	Subsonic Pressure and Velocity Profiles in the Vicinity of the Base	29
4	Details of Heat Transfer Gage	30
5	Comparison of Base Pressure Coefficient with Data of Ref. 7	31
6	Base Pressure Distribution - Supersonic	32
7	Recirculation Zone Recovery Temperature - Comparison of Present Data with Other Experimental Results	33
8	Comparison of Heat Transfer Results at the Shoulder with Prediction of Ref. 8	34
9	Base Heat Transfer Results without Injection (Supersonic)	35
10	Results of Concentration Measurements - Supersonic	36
11	Results of Concentration Measurement - Subsonic	37
12	Effect of Injection on Base Pressure (No Combustion)	38
13	Effect of Injection on Recovery Temperature (No Combustion)	39
14	Shadowgraph of Base Flow Region with and without Injection	40
15	Correlation of Effects of Injection with Concentration in the Recirculation Zone (No Combustion)	41

LIST OF FIGURES (cont'd.)

<u>Figure No.</u>	<u>Title</u>	<u>Page No.</u>
16	Direct Photograph of Base Region with Combustion in the Recirculation Zone	42
17	Effect of Combustion on Base Pressure (Supersonic)	43
18	Effect of Combustion on Recovery Temperature (Supersonic)	44
19	Effect of Combustion on Base Heat Transfer (Supersonic)	45
20	Correlation of Base Pressure and Heat Transfer with Concentration in the Recirculation Zone (Combustion)	46
21	Comparison of Measured Recovery Temperature with Adiabatic Temperature T_f	47
22	Effect of Base Heating on Recovery Temperature	47
23	Base Heat Transfer Results with and Without Combustion - Supersonic	48
24	Correlation of Base Heat Transfer Results - Supersonic	49
25	Variation of Heat Transfer Coefficient with Base Pressure (No Injection)	50
26	Subsonic Heat Transfer Results	51
27	Comparison of Supersonic and Subsonic Results for Base Heat Transfer	52
28	Effect of Combustion on Base Pressure (Subsonic)	53

LIST OF SYMBOLS

C_{p_B}	$(2/\gamma M_s^2) (p_B/p_s - 1)$ - Base pressure coefficient
c_p	Specific heat
D_T	Tunnel test section diameter
h	enthalpy, heat transfer coefficient
k	thermal conductivity
\dot{m}	mass flow rate
M_s	• Mach number at shoulder
Nu_B, \bar{Nu}_B	Nusselt numbers at base (see Equations (1) and (3))
Nu'_s	Nusselt number at shoulder based on reference enthalpy (See Equation 1)
p	pressure
Pr	Prandtl number
q_w	Heat transfer rate
Re, \bar{Re}	Reynolds number at base (see Equations (2) and (3))
Re'_s	Reynolds number at shoulder based on reference enthalpy (see Equation 1)
Re_s	Reynolds number at shoulder based on local external conditions
r_B	base radius
R	gas constant for air
T	temperature
u	velocity
X_{H_2}	measured mole fraction of hydrogen

•

LIST OF SYMBOLS (cont'd.)

\bar{X}_{H_2}	estimated mole fraction of hydrogen
x_B	model length - throat to base
x_i	injection station
γ	specific heat ratio
μ	viscosity
ρ	density

Subscripts

aw	adiabatic wall conditions
B	base properties
f	conditions evaluated at adiabatic flame temperature
H_2	fuel conditions
o	stagnation conditions
s	shoulder properties
T	tunnel conditions
w	wall conditions

"EXPERIMENTAL DETERMINATION OF HEAT TRANSFER DUE
TO HYDROGEN COMBUSTION IN A BASE FLOW REGION"

I. INTRODUCTION

During the launch phase of a certain class of space boosters venting of the fuel tanks is required in order to relieve the pressure rises caused by the aerodynamic heating. This dumped fuel may be entrained in the base region and, depending on flow conditions, combustion can ensue with subsequent exposure of the vehicle surfaces to excessive heating rates. At the present time adequate analytic methods for describing the fluid mechanics in this recirculation zone and the effect thereon of chemical reaction are not available, particularly for the case of a turbulent boundary layer at the shoulder immediately upstream of the base. Therefore, experimental results are required not only for design purposes but also to provide a framework on which to assess the validity of any future theoretical work.

To supply some fundamental data from which engineering estimates could be obtained an experimental study of this phenomenon has been carried out at the General Applied Science Laboratories. For this purpose a series of tests at Mach 3 were conducted in which the situation described above was approximated. To assess the effect of Mach number additional tests at subsonic speeds were also performed. The venting of the fuel was simulated by the tangential injection of gaseous hydrogen upstream of the base of an axisymmetric body. The specific objectives of this investigation were to establish the conditions under which combustion would occur in the recirculation region and to determine quantitatively the effect of this combustion on the pertinent base parameters. Finally these effects were to be related to, and estimated from conditions prevailing prior to the onset of combustion.

The existence of a turbulent boundary layer at the shoulder of the model was assured by the tunnel stagnation conditions used in the tests. For the Mach 3 tests these were 1000-2650°R and 130 to 440 psia for stagnation temperature and pressure respectively yielding a Reynolds number range of 3.0 to 30×10^6 based on a model length of 1.5 feet. The corresponding Reynolds number for the subsonic tests was 2.1×10^6 . These operating conditions also include temperatures sufficiently high to cause autoignition of the injected hydrogen. At the lower temperatures, since natural ignition did not occur, measurements of fuel concentration in the recirculation zone were obtained in order to define the frozen flow field that exists prior to the onset of combustion. The possibility of ignition occurring at low temperatures by virtue of local hot spots was investigated by utilizing artificial ignition devices. Both electrical spark discharges and a pyrophoric fuel pilot flame was used for this purpose. In this connection the results of Townend (Ref. 1) and Baker et al (Ref. 2) may be cited. These investigators found that stable combustion of hydrogen could be established in the base region of cylindrical bodies by artificial means at air temperatures well below practical autoignition values. These experiments were conducted at Mach numbers 2.14, and 1.6 respectively which are intermediate to those used in the present test case.

In the sections which follow the experimental equipment and procedures are first described. Then the results of tests both with and without combustion are presented and discussed. It is demonstrated that the concentration of unburned fuel in the base region is a suitable correlating parameter for describing this phenomenon. In the section the efforts to induce combustion at the lower temperatures is described. It is noted here that these efforts proved unsuccessful at Mach 3 although no difficulty was encountered in the case of the subsonic runs. Finally, a procedure for estimating the recovery temperature and heating rates associated with combustion is presented.

II. DESCRIPTION OF EXPERIMENTAL EQUIPMENT

A. High Temperature Air Supply

Two sources of high temperature air were utilized in these experiments. For tests in the lower temperature range (1000°R - 1800°R) and for tests in which concentration measurements were made, the GASL convection heater was utilized. This facility heats dry air by passing it through a bed of hot aluminum oxide pebbles. A more detailed description of this heater may be found in Reference 3. For tests at higher temperature (up to 2600°R) the GASL combustion heater was utilized. Here heating of the air stream is accomplished by burning a stoichiometric mixture of oxygen and hydrogen. This facility was previously described in Reference 4. As a result of this combustion the air stream is vitiated to a varying extent (depending on the amount of hydrogen burned to obtain a specific total temperature) due to the presence of water vapor. This effect is manifested in a variation of the specific heat ratio and must be accounted for in the nozzle design. Furthermore, the presence of water vapor tends to obscure concentration measurements which utilize a binary technique to determine the percent of species present. For this latter reason the convection heater was utilized exclusively for determination of fuel concentration in the base region.

An additional characteristic of the combustion heater is the unsteadiness of the starting process due to the manner in which combustion is initiated. This is accomplished at reduced flow rates of air and hydrogen until ignition is obtained whereupon the gas flows are increased until the desired operating conditions have been attained. The resulting unsteady history of total temperature and pressure to which the model is exposed dictates the use of a transient technique for the measurement of heat transfer as described in section D-3.

B. Sampling Equipment

The percent of injected fuel present in a typical sample of fluid collected was established by utilizing the sampling equipment which is available at GASL. The rig consists basically of a mobile, 20 bottle collecting unit and an analyzing unit which evaluates the percentage of species present in the (binary) mixture. The latter incorporates a so-called thermal conductivity cell which compares the thermal conductivity of the unknown mixture to that of premixed samples of known concentration. The required calibrations were carried out immediately before each sampling run. A detailed description of this equipment including the underlying theory, the operating procedure, and its accuracy and limitations may be found in Reference 5.

C. Nozzle and Base Model

These items are described here concurrently since the base model, including its support, forms an integral part of the annular, axisymmetric nozzle used in these tests. A schematic of the configuration is shown in Figure 1. Nozzle contours were calculated for Mach 3 flow utilizing a specific heat ratio of 1.35 which was deemed a reasonable average value over the range of stagnation temperature used in these tests. The physical area ratio which resulted corresponds to Mach 3.08 flow for pure air (i.e., for $\gamma = 1.4$). Once the general contours had been generated, an annular stream tube was selected with inner and outer diameter consistent with the mass flow capabilities of the high temperature air facilities described previously. The contour of the inner streamtube was utilized to generate the centerbody support and cylindrical base. The resulting test section diameter is nominally six inches with a cylindrical centerbody 3 1/2" in diameter at the base. In addition to eliminating

interference from a support system this approach also permits the use of a relatively large base model (for a given test section diameter) since bow shocks are not present and tunnel interference due to reflection of these waves does not occur.

The rig described here was also utilized in several subsonic runs. Subsonic flow was attained by reducing the mass flow through the nozzle. To minimize non-uniformities in the flow stainless steel screens were installed upstream of the test section as shown in Figure 1.

Injection of the gaseous hydrogen fuel was by means of either an annular slot .050 inches high or through a series of ten .040 inch I.D. tubes arranged peripherally around the cylindrical centerbody. The exit station for the fuel was located at a point approximately one base diameter upstream of the base as shown in Figure 1. Injection was essentially parallel to the model axis.

D. Instrumentation

1) Pressure Measurements

The base of the model was provided with a series of flush pressure taps .040 in. in diameter and located as shown in Figure 2. Additional static taps were installed in the tunnel wall at stations immediately upstream and downstream of the base. Free stream pitot pressures were obtained by means of small diameter (.0625 in.) total head probes supported from the tunnel wall. Care was taken in locating these to insure that the presence of the probe did not affect the base flow. For the determination of the subsonic velocity profiles shown in Figure 3 a standard Prandtl type pitot-static probe as manufactured by the United Sensor & Control Corporation (Hartford, Conn.) was utilized.

Pressures were measured with strain gauge and variable reluctance transducers; the outputs being recorded on high speed multi-channel oscillographs. A "Scanivalve" (trade name of Scanivalve Co., San Diego, Calif.) was used to manifold a number of pressures to a single transducer.

2) Temperature Measurements

The total temperature of the main stream was obtained by means of either platinum-rhodium or chromel-alumel thermocouples permanently installed in the plenum chamber of the particular facility utilized. For measurement of the recovery temperature in the recirculation zone a bare thermocouple junction was located at a point slightly off the axis and approximately 0.125 inches above (downstream) the base surface by extending the thermocouple out from the centerbody. This thermocouple was fabricated from a standard Thermo Electric Co., (Saddlebrook, N.J.) "Ceramo" thermocouple lead with an .040 in. outside diameter shield and 36 gage chromel-alumel wire. The resulting (welded) junction is quite small and insures good response with a minimum of disturbance to the base flow. The outputs from the thermocouples were recorded on oscillographs or mechanical recorders.

3) Heat Transfer Measurements

The transient heat transfer rates were obtained by means of one-dimensional gages, first described in Reference 21. Several of these gages were located in the base as shown in Figure 2. One additional gage was installed in the outer tunnel wall at a streamwise station coincident with the base shoulder (see Figure 1).

Details of the gage construction are given in Figure 4. They consist essentially of a metal plug or cylinder imbedded in the model wall in such a way as to minimize lateral heat conduction. This is accomplished by providing an insulating air gap between the cylinder and the wall of the model for most of the length of the gage. Thermocouple leads are threaded through the center of the plug and a junction is made at the surface by means of pins made of identical material. Data reduction is further simplified by making the wall thickness sufficiently large so that a semi-infinite heating situation is approximated.

The measured surface temperature history obtained with these gages is interpreted as the boundary condition for the one-dimensional unsteady conduction of heat to a semi-infinite solid (with constant thermal properties) initially at a uniform temperature. The heat transfer is obtained by numerical integration using the GASL computer program described in Reference 6.

The technique described here will generally yield values of heat flux which are lower than those actually occurring. This is due, first of all, to lateral heat conduction. Secondly, the effective location of the thermocouple junction will tend to be beneath the actual surface so that lower temperatures will be recorded thereby decreasing the estimated heat flux. Taking into account these effects, it is estimated that the measured heat flux rates will be lower than the actual values by about 5% - 15% with the error increasing at the higher temperatures.

4) Concentration Measurements

Samples of the fluid in the base region were collected by manifolding three of the five flush pressure taps located in the base to an evacuated sampling bottle. This manifolding was necessitated by the short duration of sampling time (5-10 seconds) and the low driving pressure (2-3 psia) which was available for providing a sample sufficient for an accurate analysis to be performed. The particular set of pressure taps connected to the sampling bottle was varied from time to time to ascertain the extent to which the base concentration varied along the base surface. No measurable difference could be detected. It is concluded that, within the accuracy of these measurements, the concentration in the vicinity of the base was essentially uniform.

5) Mass Flow Measurements

Mass flow measurement was by means of standard venturi meters, with the pressures being recorded by the transducer-oscillograph link described previously. In addition to the fuel injected through the model the tunnel air flow as well as the oxygen and hydrogen flow for the combustion heater were also monitored. The latter measurements are essential since they permit a comparison to be made between the measured total temperature and the theoretical flame temperature implied by the amount of fuel actually injected. These comparisons indicated that the presence of unburned hydrogen in the resulting tunnel flow was negligible.

III. PRESENTATION AND DISCUSSION OF RESULTS

A. Description of the Basic Flow

For the purpose of comparison with the results obtained with injection, considerable effort was devoted to collect measurements defining the basic flow field occurring without injection. These data are summarized in this section. In addition, wherever possible, they have been compared with available theory and/or other experimental data in order to provide a basis for assessing the accuracy of the experimental setup and measuring techniques utilized in this investigation.

1. Subsonic Tests

The nominal operating conditions for the subsonic test series are listed in Table I. Typical velocity and total pressure profiles at and near the base shoulder are shown in Figure 3 together with spacewise distributions of static pressure in the vicinity of the base. From these data it appears that the base pressure coefficient and Mach number for the subsonic tests are approximately 0.2 and .23 respectively.

2. Supersonic Tests

a. Base Pressure

The stagnation conditions for these tests are summarized in Table I. Based on a nominal centerbody length of 1.5 feet and the given data the minimum Reynolds number was 3×10^6 and in general was substantially higher than this value. Hence, the boundary layer at the shoulder was probably turbulent. This conclusion is supported by the base pressure data shown in Figure 5. As can be seen the measured results agree well with the turbulent data compiled in Reference 7. Note that the vibration of the air stream produced by the compressor motor is reflected in this data by a

slight variation in the external Mach number at the shoulder. Representative data showing the spacewise distribution of the pressure on the base during a given run is shown in Figure 6. Some variation is evident with the pressure at the axis of the base being somewhat higher than the value closer to the shoulder. For the purposes of these experiments this variation is not considered significant and the base pressure in the further discussion will be characterized by a single value corresponding to a suitable average.

b) Recovery Temperature

The results of the base recovery temperature measurement without combustion are presented in Figure 7 where they are compared with some other data available in the open literature. This data is the result of near wake investigations conducted at a variety of flow conditions as indicated in Figure 7. The comparison is made only for the purpose of establishing that the results obtained in the present test series are reasonable. There is no intent here to formulate correlations for general usage. Such an endeavor would clearly be beyond the scope of the present work.

c) Heat Transfer Results at the Base Shoulder

It was previously noted that a heat transfer gage was installed flush with the outer tunnel wall at a streamwise station coincident with the base shoulder. Although this gage is not actually located on the centerbody proper the measurements obtained there can be interpreted as applicable to the base shoulder since both locations are exposed to the same external conditions. Furthermore, for the turbulent flow conditions existing here the effect of lateral curvature is slight and corrections to account for the difference in radius are negligible. Thus, in the further discussion all measurements obtained at this location will be considered properties at the base shoulder and will be denoted by subscript s.

The heat transfer results at the shoulder are shown in Figure 8. To assess the accuracy of these measurements the results have been compared with the prediction of the flat-plate reference enthalpy method (cf Method I of Ref. 8) denoted henceforth as the FPRE method. According to this method the heat transfer can be predicted from the relation

$$Nu'_s = 0.03 (Pr')^{1/3} (Re'_B)^{4/5} \quad (1)$$

where

$$Nu'_s = \frac{q''_s x_B k'}{c_p' (h_{a_w} - h_w')}$$

$$Re'_B = \rho' u_{e_B} x_B / \mu'$$

$$Pr' = \mu' c_p' / k'$$

Here primed quantities denote thermodynamic properties of the fluid which are evaluated at the reference enthalpy defined by

$$h' = 0.5 h_{w_s} + 0.22 Pr^{1/3} h_{o_T} + h_{e_s} (0.5 - 0.22 Pr^{1/3}) \quad (2)$$

The reference length x_B used in the calculation was taken as the axial distance from the throat of the nozzle to the base. The data are seen to be generally below the values predicted by Equation (1). Part of this difference can be associated with errors inherent in Equation (1) itself which is strictly valid only for zero pressure gradient. In general, it has been found (cf. Ref. 9) that the FPRE method will yield values which are high in the case of a favorable pressure gradient which prevails in a nozzle. Thus agreement can be considered good for tests in the convection heater but only fair in the case of combustion heater data. The distinct shift in magnitude

exhibited by the latter is systematic and hence probably not due to experimental scatter. Corrections were performed to account for the presence of water vapor but these proved to be negligible. The behavior is probably due to the lateral conduction effects in the heat transfer gage previously mentioned, which increase not only with higher heating rates but also with increased running time. Note that uniform conditions were achieved in the convection heater within 2-3 seconds whereas, as a rule, approximately 10-12 seconds elapsed before the combustion heater was operating at the desired steady state.

d) Heat Transfer Results at the Base

The heat transfer results at the base without injection are shown in Figure 9 in non-dimensional form according to:

$$\begin{aligned} \text{Nusselt Number} \quad Nu_B &= q_{w_B} r_B / (k_{O_B} (T_{O_B} - T_{w_B})) \\ \text{Reynolds Number} \quad Re_B &= p_B h_{O_B} r_B / \mu_{O_B} \quad (3) \end{aligned}$$

where the thermodynamic properties are computed from standard air tables for the measured value of T_{O_B} . The values of heat transfer rate used are those occurring during steady state with the wall temperature and base pressure at the corresponding instantaneous values. Each data point corresponds to a particular test run and for each of these the heat flux has been characterized by a single value of q_{w_B} since, as in the case of the base pressure measurements, spacewise resolution was deemed not meaningful within the present experimental accuracy. The value utilized represents the maximum of the several available.

The data again exhibits the behavior previously observed at the model shoulder in that the results obtained in the convection heater are systematically higher. However, this effect is considerably less pronounced as would be expected for the lower heating rates occurring at the base.

As indicated in Figure 9 the heat transfer results exhibit a Nusselt number dependence on the $2/3$ power of Reynolds number. This is in agreement with the conclusions of Reference 10 and 11 wherein the heat transfer characteristics of turbulent separated flows have been examined.

B. Concentration Measurements

In tests where concentration measurements were obtained, tunnel and fuel flow were initiated simultaneously. However, sampling of the fluid in the recirculation zone was delayed a minimum of 2 seconds to assure the existence of steady conditions in the base. This delay was automatically controlled by electrical timers activated by initial fuel injection. The sampling was accomplished by the procedure previously described.

The results of concentration measurements are summarized in Figures 10 and 11 for the supersonic and subsonic tests respectively. In these figures the mass flow of hydrogen has been non-dimensionalized with respect to the overall tunnel mass flow. This method of normalizing the results is chosen for convenience in interpreting the data obtained with combustion as will be described in a later section.

The dependence of the base concentration of fuel on the mode of injection as well as on the rate thereof is clearly evident for both the subsonic and supersonic runs. This behavior is probably associated with the difference in the mixing mechanism which exists between the two injection schemes.

Clearly the higher base concentrations are associated with greater entrainment of fuel in the recirculation zone which in turn implies less mixing of the fuel with the high velocity external air capable of traversing this region. Hence, it would appear that much greater mixing occurs with tubular injection which is of course, consistent with the three-dimensional character of this configuration. The efficiency of the process with annular injection is even further reduced because of the possible laminarization of the boundary layer on the cylinder due to the low exit velocities.

C. Effect of Injection on Base Parameters in the
Absence of Combustion

The effect of fuel injection on base pressure and recovery temperature is shown in Figures 12 and 13 for the supersonic case. Corresponding results for the low speed tests are not presented since no discernible effect on these parameters was observed. However, it should be noted that the reduction in the recovery temperature is a consequence of the low temperature of the fuel relative to the free stream air. Thus, for the subsonic tests where both fuel and free stream air were at ambient temperature no decrement in recovery temperature would be expected.

The trends previously observed for base concentration are reflected once again in the data taken in the recirculation zone. That is, a substantially greater effect is produced by the annular

mode of injection on both pressure and temperature at any given rate of fuel flow.

• Insofar, as the temperature effect is concerned it is clear that this is associated with the entrainment of cold hydrogen in the recirculation zone. Despite these lower temperatures however, the low molecular weight of the entrained fuel would tend to reduce the average density in the streamtube contained by the dividing streamline. From a fluid dynamic point of view this would be reflected in a reduction in the expansion suffered by the dividing streamtube with a consequent increase in the equilibrium pressure within the dead air region. This effect is demonstrated in the observed pressure rises and by the shadowgraph pictures of the base flow shown in Figures 14. Here, the flow patterns with and without injection have been compared. An increase in the neck diameter at the point where the recompression shocks begin can be seen in the injection case.

If the argument presented above is correct it follows that the observed effects on base pressure and temperature should be uniquely related to the amount of injectant entrained and independent of the mode of injection. A correlation of these effects with the measured concentration has been made and is presented in Figure 15. Suppression of the injection mode as a parameter is clearly evidenced by these results. This property proves to be of considerable utility in the interpretation of the results obtained with combustion.

D. Effect of Combustion

1. General Remarks

Although no difficulty was encountered in inducing combustion artificially at low flow temperatures during the subsonic tests, similar efforts at Mach 3 proved fruitless. In the latter case both

electrical spark discharges and a triethylaluminum (TEA) pilot flame were utilized as ignition sources. The TEA pilot flame was established directly in the base flow region by injecting the pyrophoric through one of the existing pressure taps. The spark, situated at a stream-wise station approximately one inch downstream of the base, was mounted on a pneumatic cylinder which could be withdrawn once combustion was initiated. The stroke of this cylinder was sufficient to traverse the entire jet from the outer tunnel wall to the model axis.

At subsonic speeds only the spark source was utilized since ignition was readily achieved in this way. This combustion persisted in a stable manner after withdrawal of the spark as long as fuel flow was maintained.

Referring now to the Mach 3 case, in tests using the spark discharge it can be stated categorically that no hydrogen combustion occurred. In the case of the pilot flame only indirect evidence that combustion was not induced can be offered since the presence of the pilot flame itself was reflected by rises in pressure, recovery temperature, and heating rates at the base. This indirect evidence is as follows. First, the observed effects persisted only so long as the TEA flow was maintained even if the hydrogen flow was continued for a longer period. Secondly, the magnitude of these effects (e. g., base pressure rise) was indistinguishable between runs which, in one case included both hydrogen and TEA flow, and in the other, only TEA flow was maintained. These efforts were carried out over the temperature range 1500-1800°R. It is concluded that for the injection configurations used and for the Mach 3 condition stable combustion in the recirculation zone cannot occur at these low temperatures. Thus, in view of the results of Townend (Ref.1) and Baker et al (Ref.2) a "flame out" Mach number exists somewhere.

between 2.14 and 3. The latter conclusion must be considered provisional however, since differences in the injection configuration existed between the present tests and the experiments cited.

For convenience in the further discussion the results obtained with combustion will be characterized as either supersonic or subsonic. In the first category will be included those tests at Mach 3 where combustion was a consequence of autoignition due to elevated flow stagnation temperatures. In the second category will be included subsonic tests where combustion was induced artificially by means of an electrical spark.

2. Supersonic Results

The procedure here consisted of first establishing the desired steady state tunnel conditions whereupon injection of the fuel was initiated by activating a system of electrically operated valves. Visual observation of the base region during the test was by means of a television monitor. The burning was readily observed, steady, and persisted so long as the fuel was maintained. A typical direct photograph obtained during burning is shown in Figure 16. The effect of this combustion on base pressure, recovery temperature and base heat flux rates is shown in Figures 17, 18, 19. Here the values obtained with combustion have been compared with the appropriate condition occurring immediately before burning was initiated. This comparison is made over a range of fuel flow with the injection mode as a parameter.

In order to correlate these effects with the concentration as for the non-burning results the concentration was estimated by utilizing the measured fuel flow rates in conjunction with the calibration curves drawn through the data shown in Figure 10. This is necessitated, of course, by the fact that direct measurement of fuel concentration was not possible during these high temperature runs. The

result of this correlation is shown in Figure 20. Again suppression of the influence of injection mode is apparent.

In a further effort to describe the observed phenomena in an elementary way the (equilibrium) adiabatic flame temperature corresponding to the estimated values of concentration and the conditions at the base prior to combustion (i.e., the frozen condition) was calculated and is compared with the measured recovery temperature in Figure 21. This procedure is in the spirit of Zakkay (Ref. 12), who has demonstrated that an accurate prediction of the flame temperature in free jets can be obtained by this technique. Of course, in the present application this procedure cannot be expected to be as accurate for two reasons. First of all, in view of the heat sink capability of the model, the process is non-isoenergetic so that an approach which neglects this effect would tend to over predict the final temperature. The existence of this effect is evidenced by the comparison drawn in Figure 21 and the data of Figure 22, showing the effect of increased heating rates on the recovery temperature and the latter's departure from the calculated value. A second reason for expecting some deviation between the calculated and measured values is, of course, associated with the pressure rises observed with burning and their resulting effect on the flow field. This interaction is especially critical in the case of a base flow. Despite these shortcomings, the procedure appears to provide a rational method for estimating the maximum temperature.

The heat transfer results obtained with combustion are compared with the no injection results in Figure 23 using the non-dimensional representation previously introduced (cf. Eq. (3)). In computing these parameters the values of T_{o_B} and p_B that occur during combustion are utilized. Then the thermal properties (μ , k , h) are

evaluated at this temperature and pressure from standard air tables. Although it would appear that a rough correlation has been obtained by plotting the data in this form it is clear that this correlation is of questionable value since it involves quantities which, at present, cannot be predicted (i.e., the recovery temperature and base pressure with combustion). In order to effect a more meaningful correlation and one which would have some engineering utility, modified definitions of Nusselt and Reynolds numbers were introduced in accordance with:

$$\overline{Nu}_B = q_{w_B} r_B / k_f (T_f - T_{w_B}) \quad ; \quad \overline{Re}_B = p_{B_i} \sqrt{h_f} r_B / \mu_f R T_f \quad (4)$$

where T_f denotes the flame temperature calculated as described before, subscript f denotes properties evaluated at this temperature and subscript i denotes conditions occurring prior to combustion. The result of this modification is shown in Figure 24. The power law correlation shown in this figure fits all of the data within $\pm 12\%$ with the exception of one of the annular combustion runs. It should be noted that the pressure rise associated with this run was the highest observed in the series, amounting to an increase approximately 75% over the initial value. This indicates that the usefulness of the correlation is restricted to those cases where modification of the flow field by the combustion is small.

Subject to this restriction, the correlation provides a method for predicting the heating rates to which the base would be exposed during combustion from a knowledge of conditions existing prior to combustion if a reasonable estimate of the concentration in the recirculation region can be made. Of course, the present results do not provide any way of making this latter estimate; on the contrary they indicate the inherent difficulty in making any such

predictions since this parameter is not simply related to flow rate but depends critically on the particular flow configuration used to introduce the fuel. On the other hand, an estimate of the maximum heating to be expected can be obtained by assuming in all cases the stoichiometric condition to prevail. As an example, consider the following set of initial data which corresponds to one of the tests described in this report. Take $p_{Bi} = 3.5$ psia, $T_{O_{Bi}} = 1320^{\circ}\text{R}$, $T_{w_{Bi}} = 632^{\circ}\text{R}$ and assume $X_{H_2} = 0.424$ (i.e., an equivalence ratio of unity). Then from combustion tables (Ref. 13) $T_f = 4640^{\circ}\text{R}$ so that $\overline{Re}_B = 3.5 \times 10^4$.
Hence,

$$\overline{Nu}_B = 0.12(3.5 \times 10^4)^{0.68} = 147$$

so that $q_{w_B} = 117 \text{ BTU/ft}^2 \text{ sec}$. This value is approximately twice the measured value of $54 \text{ BTU/ft}^2 \text{ sec}$. and the latter includes the effect of a pressure rise amounting to a 60% increase over the initial value. Hence this approach can generally be characterized as conservative.

Finally, it is noted that an upper limit in the rise in heating rate is indicated by the data. In Figure 20 it can be seen that for hydrogen concentrations approaching stoichiometric the rate of increase in heat transfer is attenuated. It is expected that for higher concentrations this trend would continue. It appears that this maximum corresponds to a factor of four. This includes a pressure effect which, if eliminated, would result in lower rates of heating due to the combustion alone. The effect of pressure on heat transfer coefficient is shown in

Figure 25. The data includes only those results obtained without injection. With this as a basis, a correction applied to the data of Figure 20 would indicate a maximum increase in heating rate approximately three times the initial value.

3. Subsonic Results

All of the test data for the subsonic tests have been tabulated in Table II. It should be noted that during this series the thermocouple monitoring the recovery temperature was inoperative. Hence, thermocouple probes were installed at two downstream stations at the model axis and at the distances given in Table II in multiples of the base radius r_B .

The heat transfer results are summarized in Figure 26 and compared with the supersonic data in Figure 27. A distinct Mach number effect is evident. It should also be noted that combustion was achieved only with the annular injection mode presumably because of the excessively dilute fuel concentration occurring with tubular injection. This agrees with the results of test 281 and 284 wherein combustion was not achieved even with the annular injector but at the lowest rates of fuel flow. It should appear that for this configuration a lower limit for combustion occurs at $X_{H_2} \approx 0.1$. This limit has been characterized in the various figures as the "flame out" limit. This agrees with the limits of inflammability established for related configurations wherein pilots and flame holders are utilized to induce ignition at similar temperature levels. The effect of combustion on base pressure is shown in Figure 28.

IV. CONCLUSIONS

On the basis of the experiments described in this report the following conclusions have been reached:

1. The appropriate parameter for correlating the effects of injection and combustion of a fuel entrained in the recirculation zone of a cylindrical base is the concentration of the fuel therein.
2. The adiabatic flame temperature calculated from the initial (frozen) condition existing prior to combustion provides a rational estimate of the recovery temperature in the recirculation zone.
3. At Mach 3, and with hydrogen as the injected fuel, the maximum increase in heating rate due to combustion is estimated to be on the order of a factor of 3 to 4.
4. At Mach 3 it appears that stable combustion in the recirculation zone will not occur if free stream total temperatures are below approximately 1800°R, even if local hot spots occur in the immediate vicinity of the base.

In addition to these conclusions a method for estimating heat transfer and recovery temperature in the base region with combustion of hydrogen has been described. This procedure involves a correlation formula which has been found to exhibit a Mach number dependence. Additional tests at different Mach numbers would be required to ascertain the form of this Mach number effect.

V. REFERENCES

1. Townend, J.H., "Some Effects of Stable Combustion in Wakes Formed in a Supersonic Stream", Royal Aircraft Establishment (Farnborough) Technical Note Aer 2872, March 1963.
2. Baker, W.T., Davis, T., and Mathews, S.E., "Reduction of Drag of a Projectile in a Supersonic Stream By the Combustion of Hydrogen in the Turbulent Wake", The Johns Hopkins University Applied Physics Lab., CM-673, June 1951.
3. Description of Experimental Facility, GASL TI-44, September, 1966.
4. Dunn, J., "Experimental Results for Thermal Ignition of Hydrogen in a Supersonic Viscous Flow", GASL TR-404, December 1963.
5. Feeley, H., "Analysis of Binary Gas Mixtures by the Thermal Conductivity Method", GASL TM No. 26, April 1965.
6. Bellow, B., "IBM Program for Computation of Aerodynamic Heat Transfer Rate for Any Measured Surface Temperature History", GASL CM33A, April 1966.
7. Love, E.S., Base Pressure at Supersonic Speeds on Two-Dimensional Airfoils and on Bodies of Revolution With and Without Fins Having Turbulent Boundary Layers", NACA TN 3819, January 1957.
8. Eckert, E.R.G., "Survey on Heat Transfer at High Speeds", Wright Air Development Center TR 54-70, 1954.

9. Cresci, R.J., MacKenzie, D.A., and Libby, P.A. "An Investigation of Laminar, Transitional and Turbulent Heat", Journal of the Aero/Space Sciences, Vol. 27, No. 6 pp. 401-414, June, 1960.
10. Richardson, P.D., Estimation of the Heat Transfer from the Rear of an Immersed Body to the Region of Separated Flow", Aero Res. Labs., Office Aerospace Res., USAF, ARL 62-423, September 1962.
11. Hanson, F.B. and Richardson, P.D., "Mechanics of Turbulent Separated Flows as Indicated by Heat Transfer", A Review, ASME Fluids Engineering Conference, Symposium on Fully Separated Flows, Phila. Pa., May 18-20, 1964, pp. 27-32.
12. Zakkay, V., and Krause, E., "Mixing Problems with Chemical Reactions", Supersonic Flow, Chemical Processes and Radiation Transfer, Pergamon Press, New York, 1964, pp. 3-29.
13. Drell, I.T. and Belles, F.E., "Survey of Hydrogen Combustion Properties", NACA Report 1381, 1958.
14. Todisco, A. and Pallone, A., "Near Wake Flow Field Measurements," RAD-TM-65-21 (BSD-TR-65-248), May 1965.
15. GASL Monthly Progress Report No. 8, Job 8339, September 1966.
16. Martellucci, A., Trucco, H., Ranlet, J. Agnone, A., "Measurements of the Turbulent Near Wake of a Cone at Mach 6," AIAA Paper No. 66-54, January 1966.
17. Martellucci, A., Schlesinger, A., "Measurements of the Laminar Near Wake of a Cone at Mach 12," GASL TR 582, June 1966.

18. Todisco, A., Pallone, A., Heron, K., "Hot-Wire Measurements of the Stagnation Temperature Field in the Wake of Slender Bodies," RAD-TM-64-32, July 1964.
19. Cresci, R.J. and Zakkay, V., "An Experimental Investigation of the Near Wake of a Slender Cone at $M_\infty = 8$ and 12," ARL 65-87, May 1965.
20. Larson, R.E., Scott, C.J., Elgin, D.R., Seiver, R.E., Turbulent Base Flow Investigations at Mach Number 3," Rosemount Aeronautical Laboratories, University of Minnesota, Research Report No. 183, July 1962.
21. Cresci, R.J., Libby, P.A., "Some Heat Conduction Solutions Involved in Transient Heat Transfer Measurements", Polytechnic Institute of Brooklyn, PIBAL Report No. 384, WADC TN 57-236 AD 130800, September 1957.

TABLE I

TUNNEL OPERATING CONDITIONS

Mach Number M_s	Stagnation Pressure P_{0T} (psia)	Stagnation Temperature T_{0T} (°R)	Unit Reynolds No. ft^{-1}
3	130 - 440	1000 - 2650	$2 - 20 \times 10^6$
0.23	30 ⁽¹⁾	520	1.4×10^6

(1) Pressure recovery through nozzle was approximately 0.5 so that total pressure in test section was essentially atmospheric.

TABLE II

SUMMARY OF SUBSONIC TESTS WITH HYDROGEN INJECTION

Run No.	Injection Config.	$\frac{\dot{m}_{H_2}}{\dot{m}_T}$	X_{H_2} (1)	P_B (psig) initial	P_B (psig) With Combustion	q_{wB} (BTU/ft ² sec)	T_{0T} (°R) $x/t_B=1.3$	T_{0T} (°R) $x/t_B=3.4$	T_f (°R)	Burning Achieved
COMBUSTION TESTS										
275	Tubular	.002	.068	-.21						No
276		.00275	.076	-.225						No
277	Annular	.0033	.166	-.24	-.11	21.4			2850	Yes
278	"	.0036	.174	-.235	-.08	24.8			2950	Yes
279	"	.0041	.204	-.215	0	27.6			3340	Yes
280	"	.0029	.156	-.23	-.117	22.6			2740	Yes
281	"	.0019	.113	-.24						No
282	"	.0022	.125	-.24	-.128	17.1	1985	1850	2300	Yes
283	"	.0022	.127	-.24	-.144	16.4	2005	1830	2350	Yes
284	"	.0018	.108	-.24						No
285	"	.0042	.222	-.24	-.006	27.9			3570	Yes
286	"	.0042	.222	-.22	+.014	27.2	2930	2930	3570	Yes
SAMPLING TESTS										
289	Annular	.0044	.225	-.23						
290	"	.0033	.18	-.22						
291	"	.0021	.126	-.25						
292	"	.0011	.07	-.26						
293	Tubular	.0069	.10	-.19						
294	"	.0032	.085	-.21						
295	"	.0021	.073	-.215						
296	"	.0011	.053	-.22						

(1) Denotes estimated values for combustion tests and measured values for sampling tests.

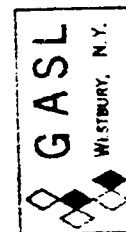
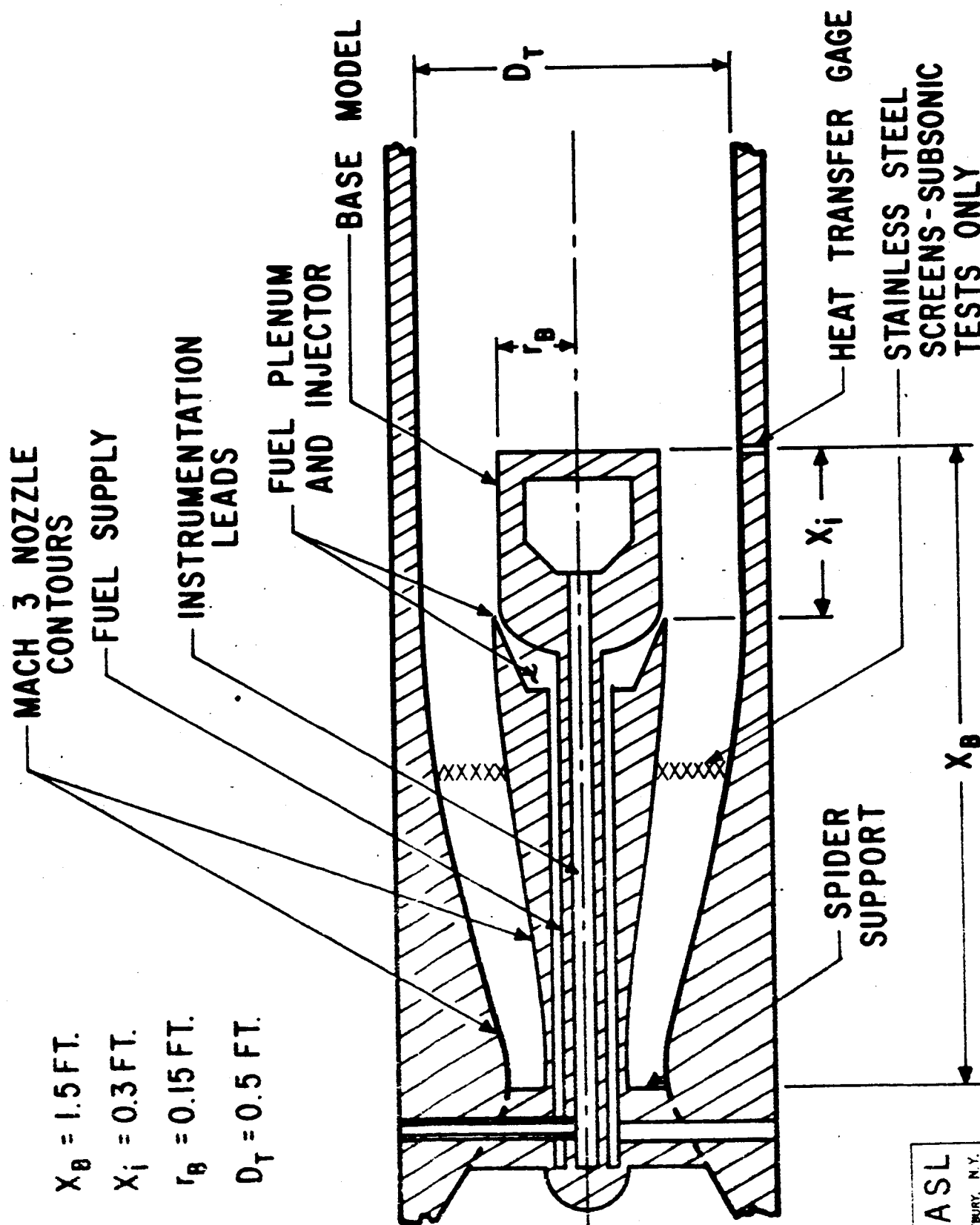


FIG. 1 SCHEMATIC OF MODEL AND NOZZLE CONFIGURATION

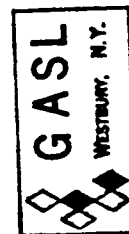
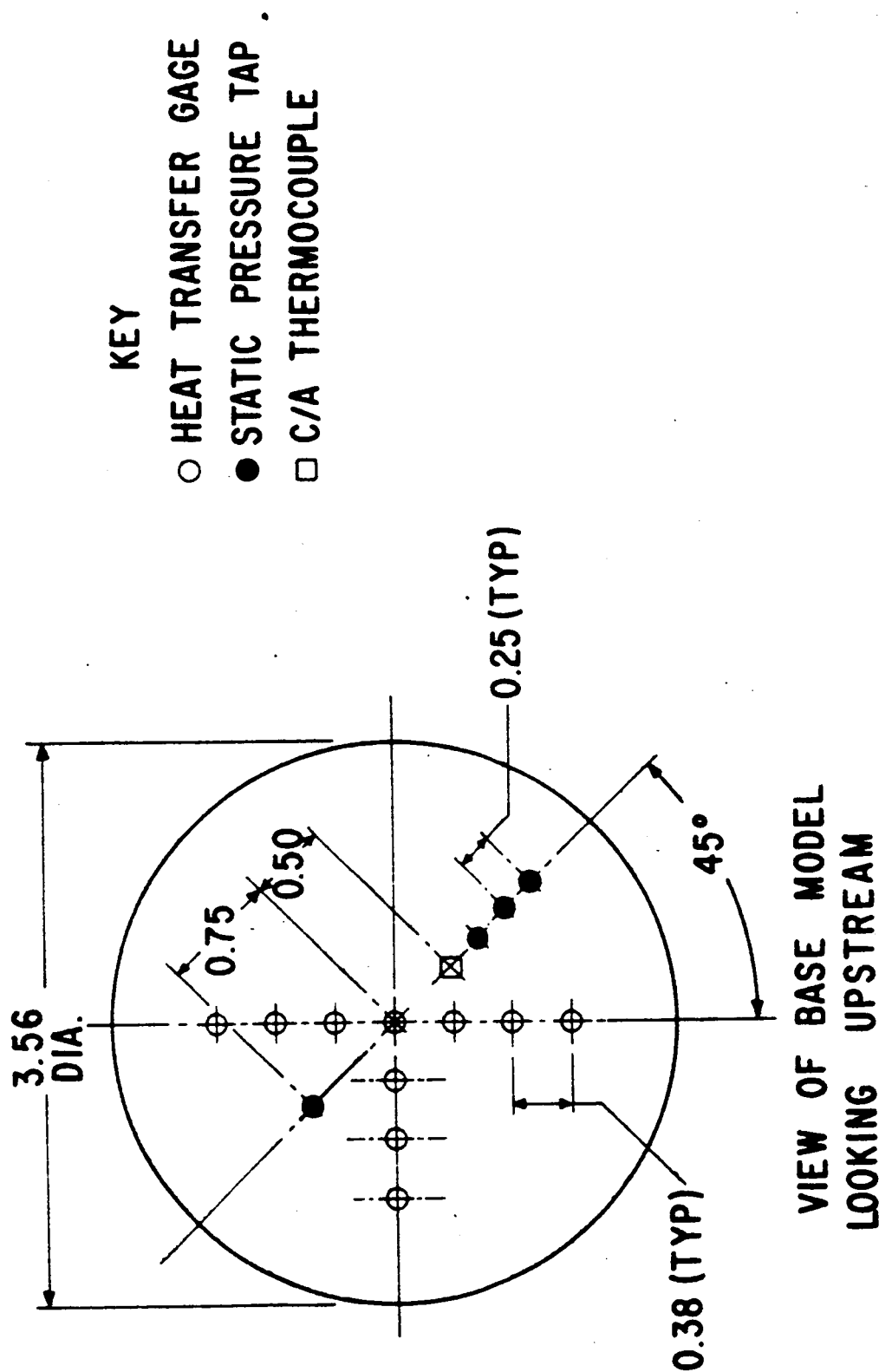


FIG. 2 LOCATION OF INSTRUMENTATION ON BASE MODEL

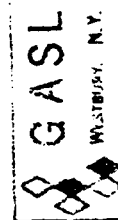
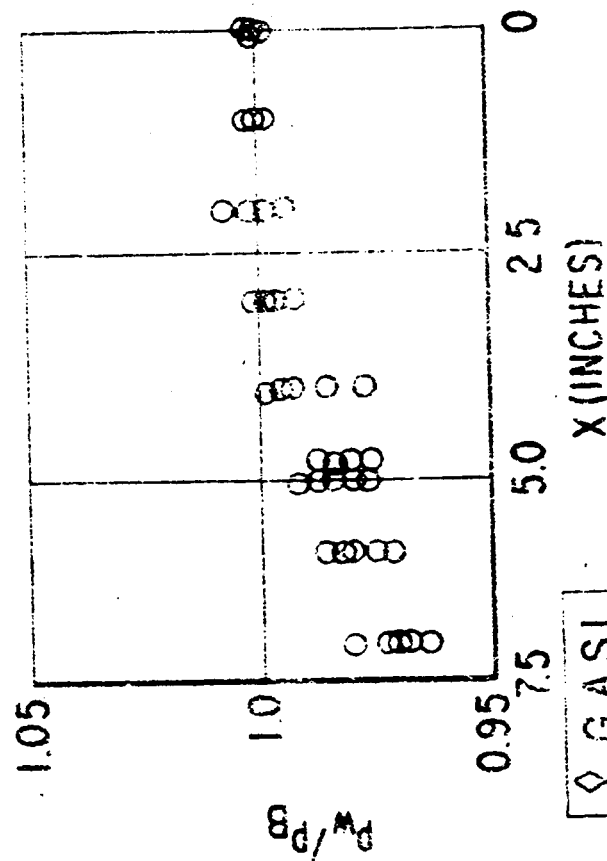
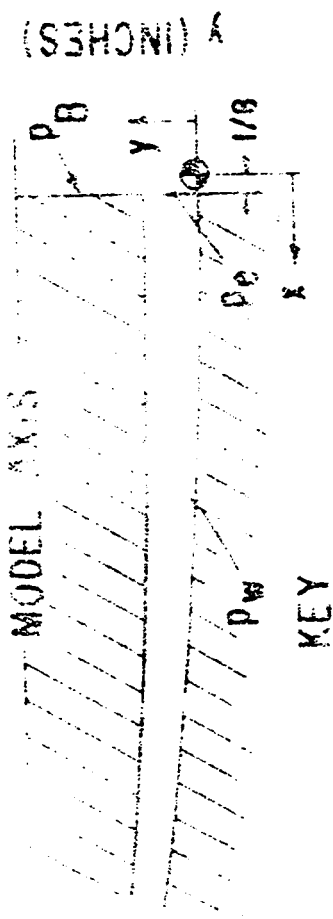
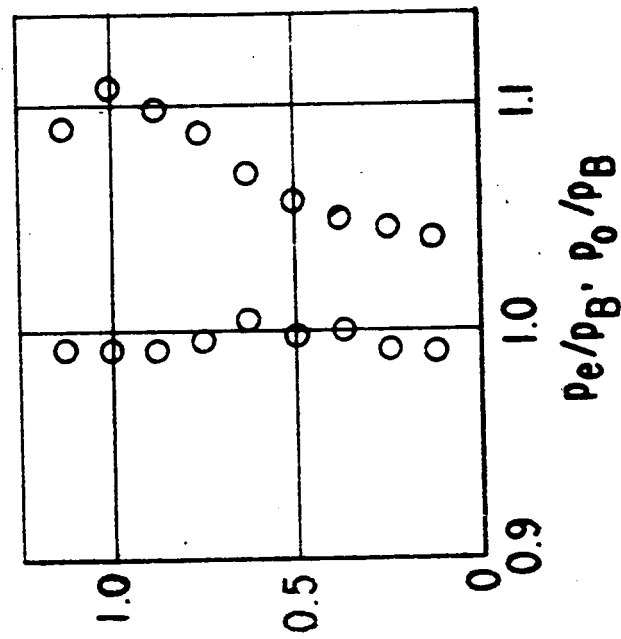
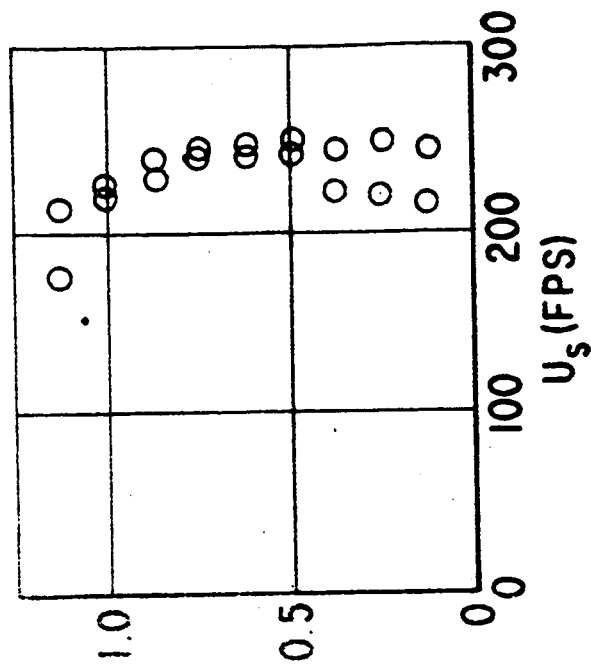


FIG. 3 SUBSONIC PRESSURE AND VELOCITY PROFILES IN THE VICINITY OF THE BASE

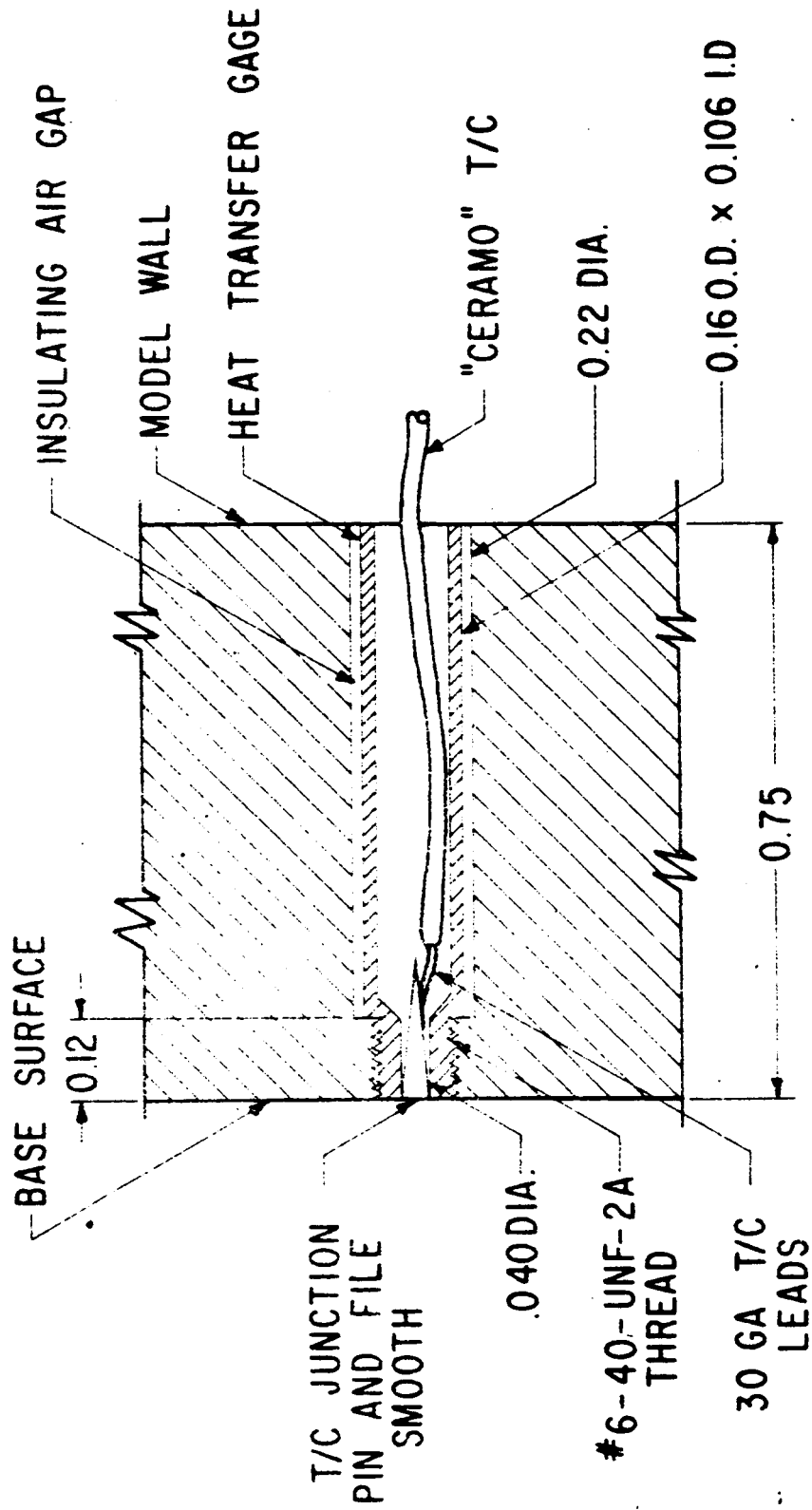
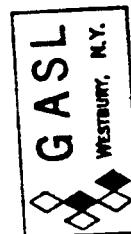
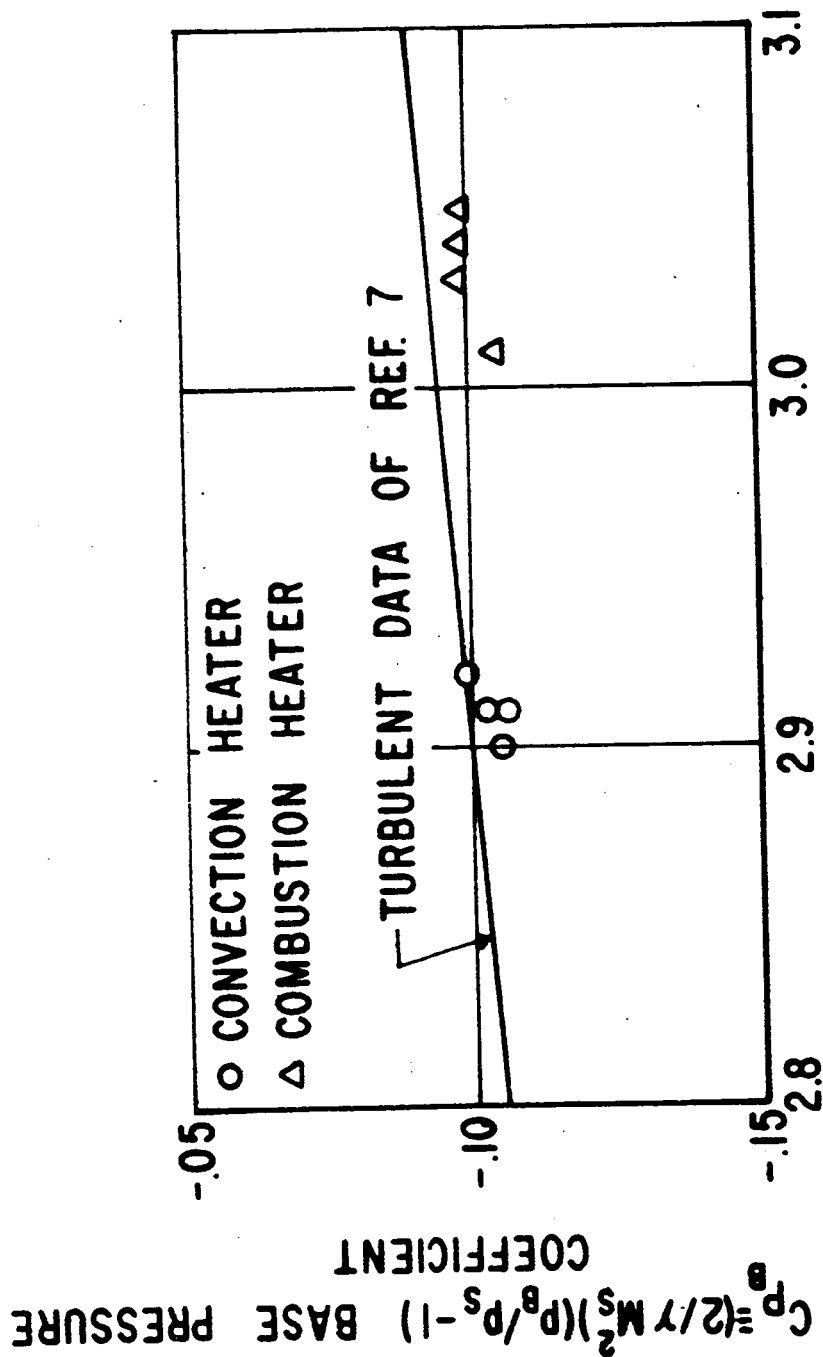


FIG. 4 DETAILS OF HEAT TRANSFER GAGE



M_s - MACH NUMBER AT THE SHOULDER

FIG. 5 COMPARISON OF BASE PRESSURE COEFFICIENT WITH DATA OF REF. 7

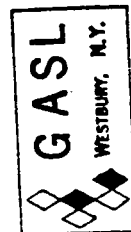
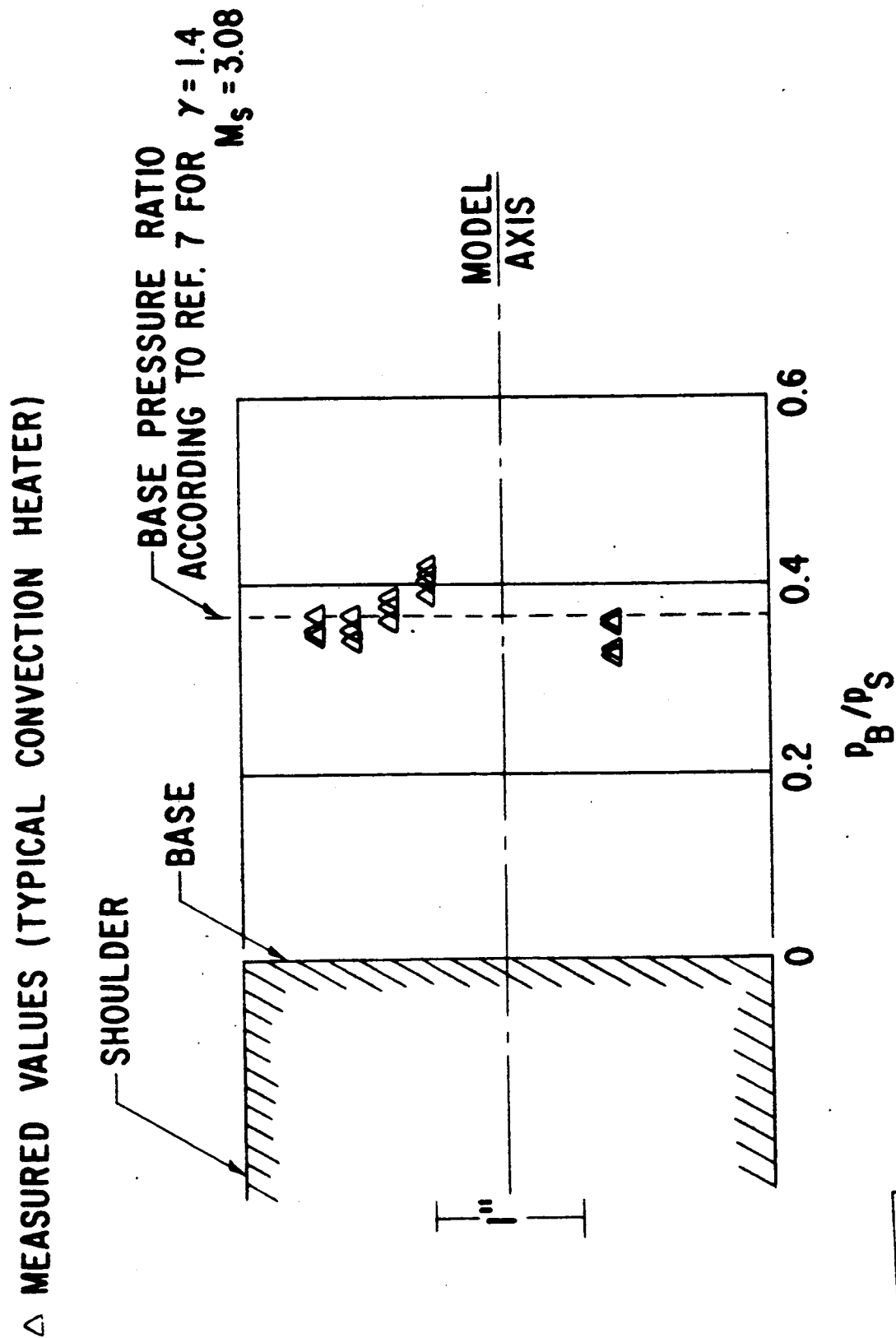


FIG. 6 BASE PRESSURE DISTRIBUTION - SUPERSONIC

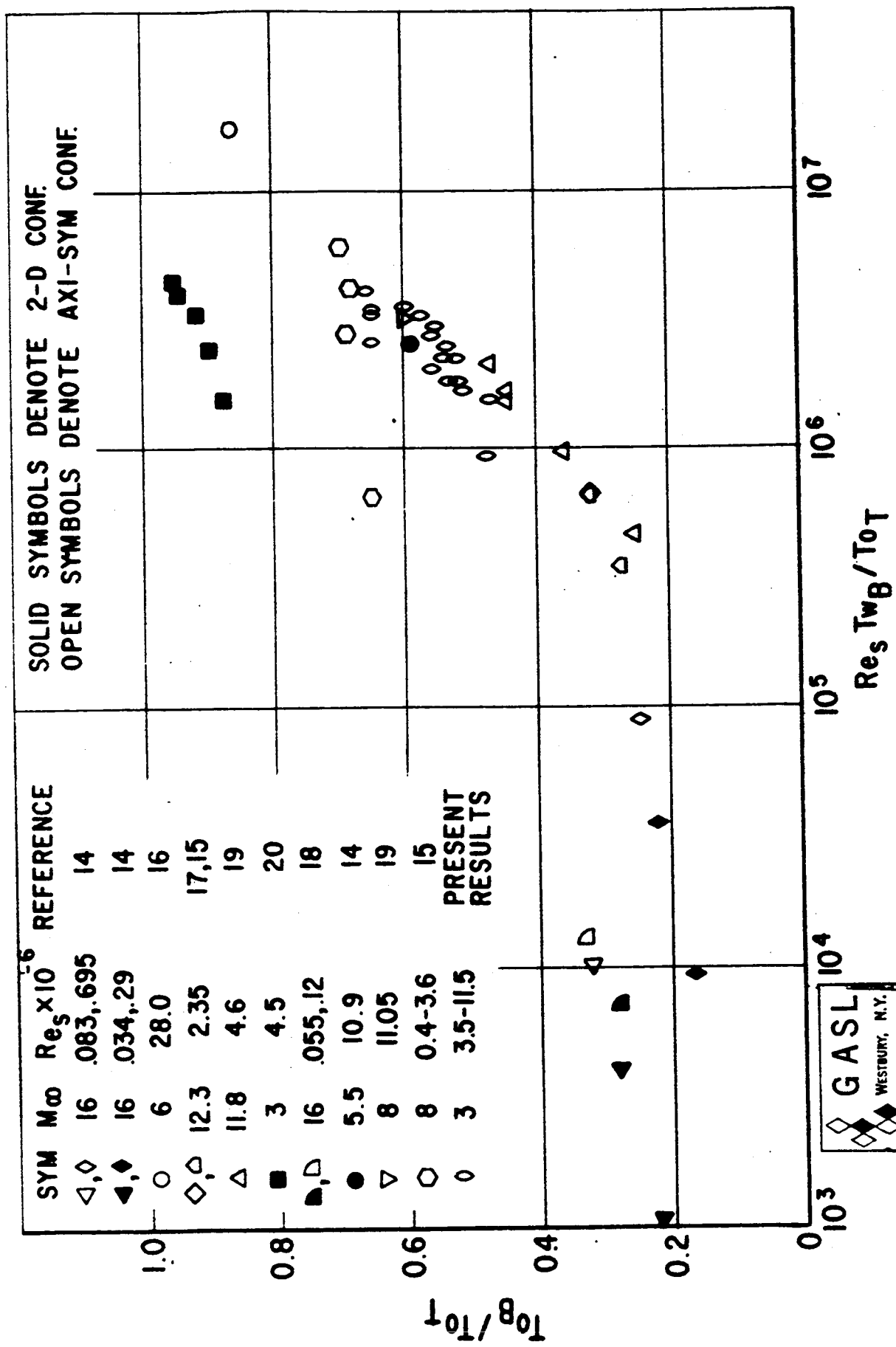


FIG. 7 RECIRCULATION ZONE RECOVERY TEMPERATURE - COMPARISON OF PRESENT DATA WITH OTHER EXPERIMENTAL RESULTS

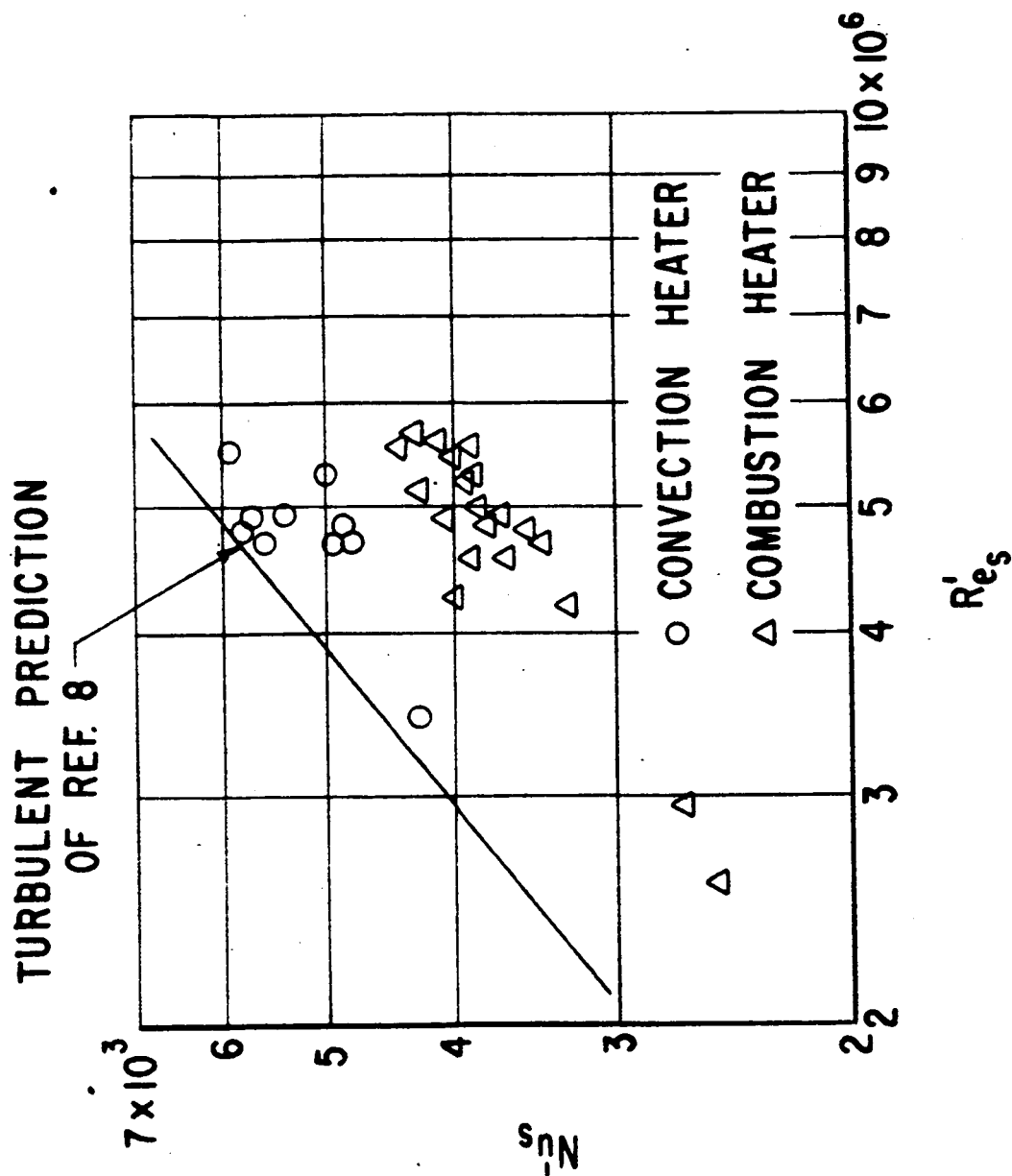


FIG. 8 COMPARISON OF HEAT TRANSFER RESULTS AT THE SHOULDER WITH PREDICTION OF REF. 8

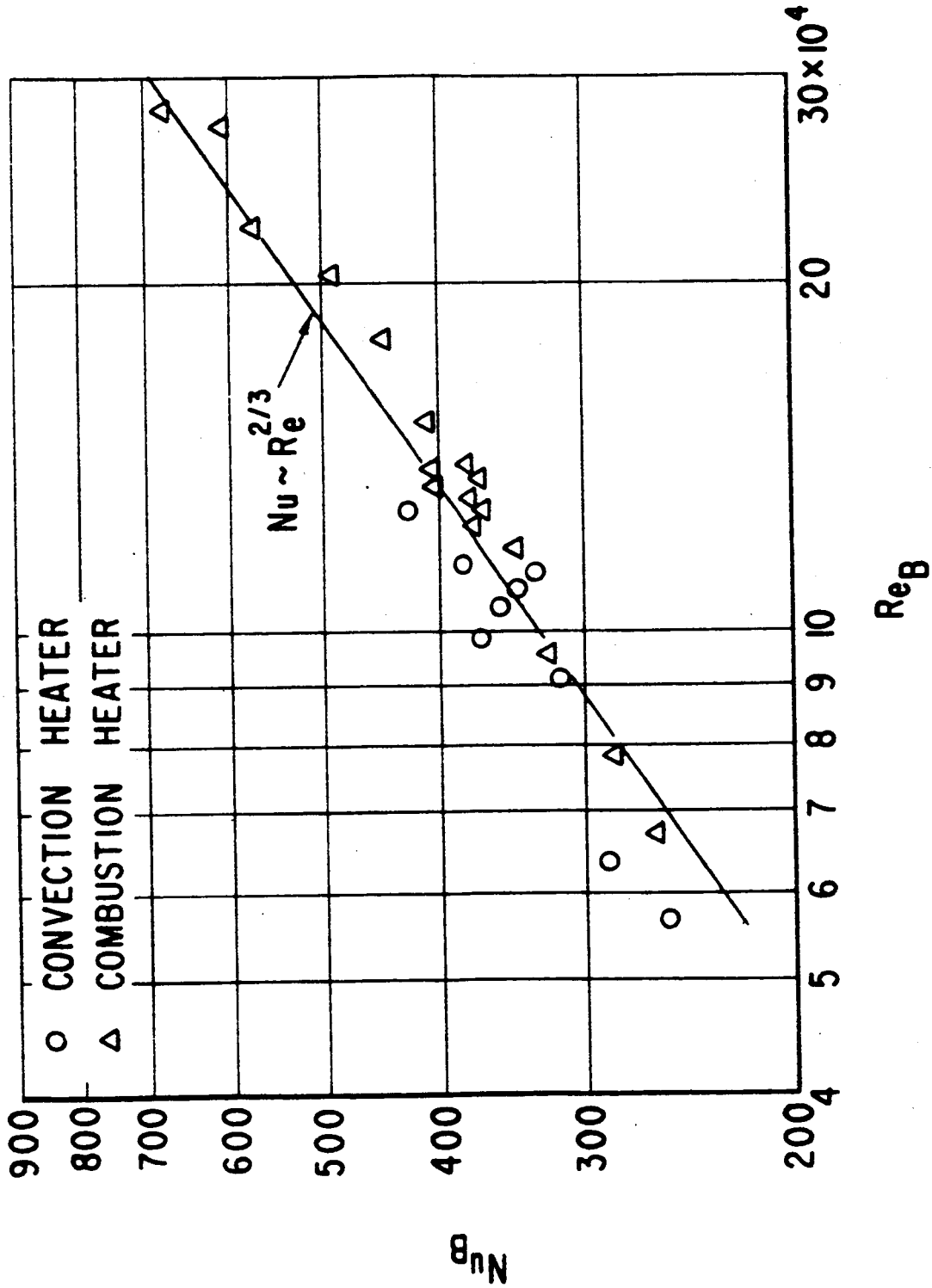


FIG. 9 BASE HEAT TRANSFER RESULTS WITHOUT INJECTION
(SUPERSONIC)

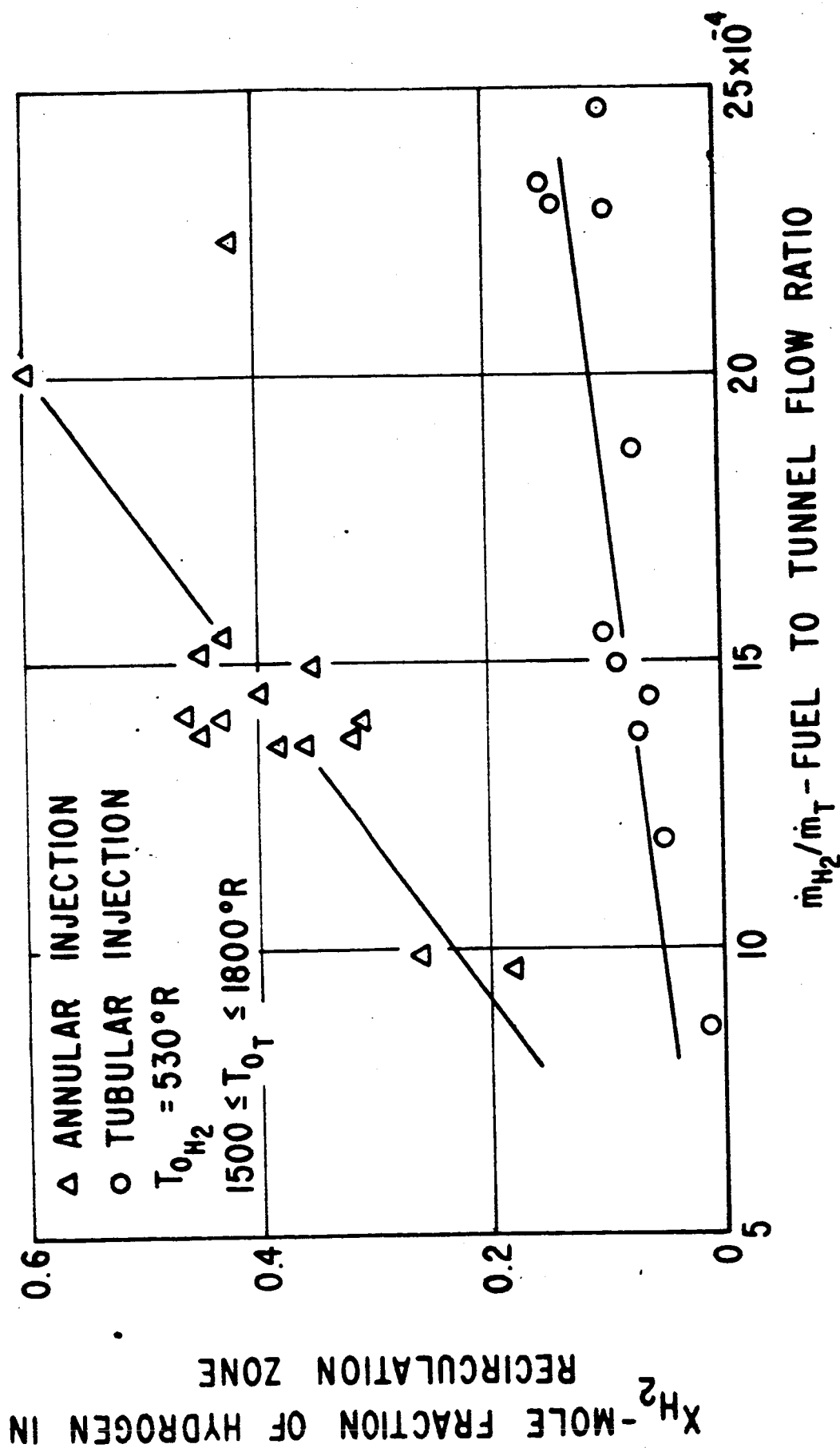


FIG. 10 RESULTS OF CONCENTRATION MEASUREMENTS - SUPERSONIC

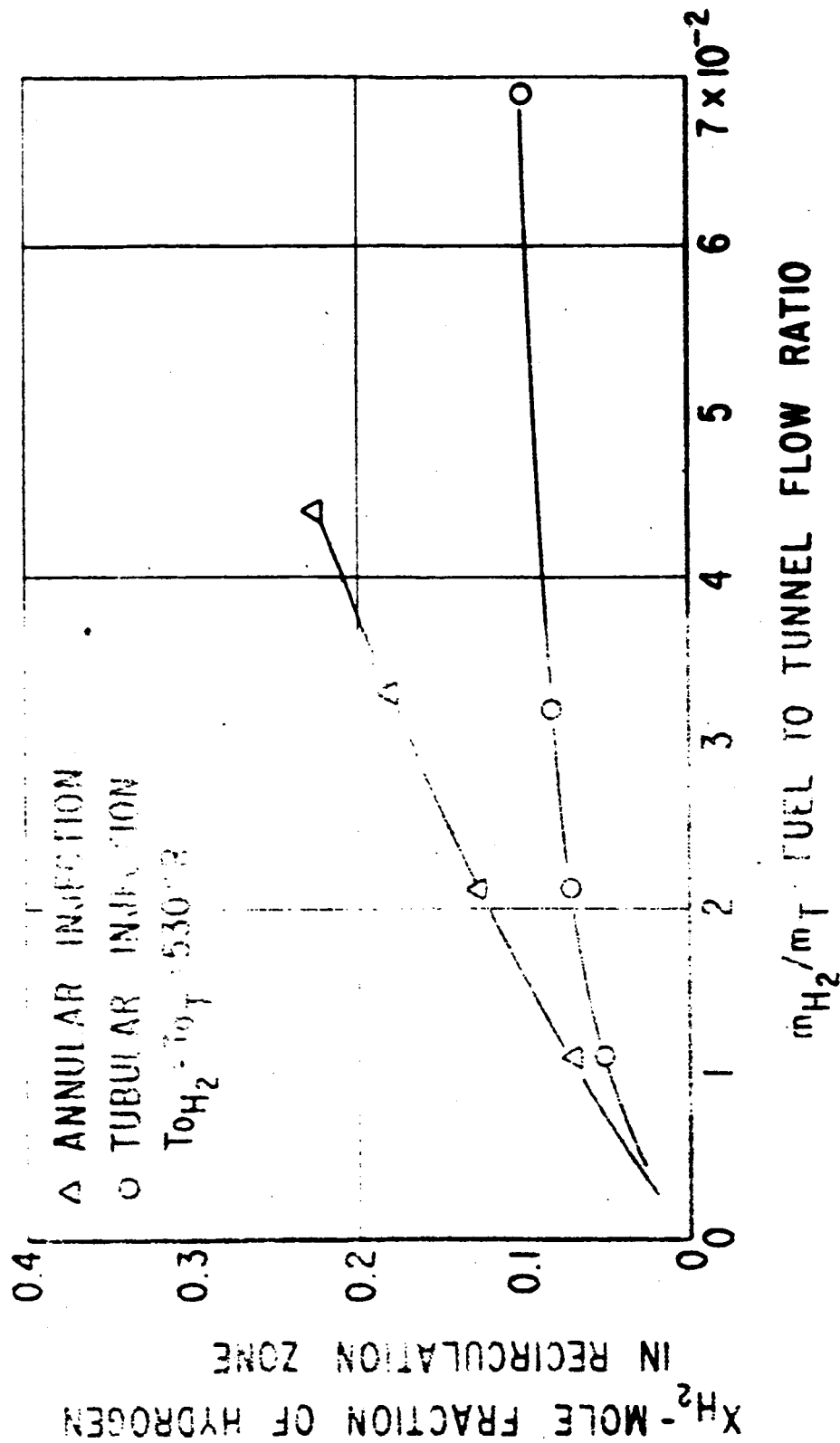
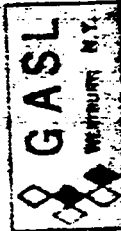
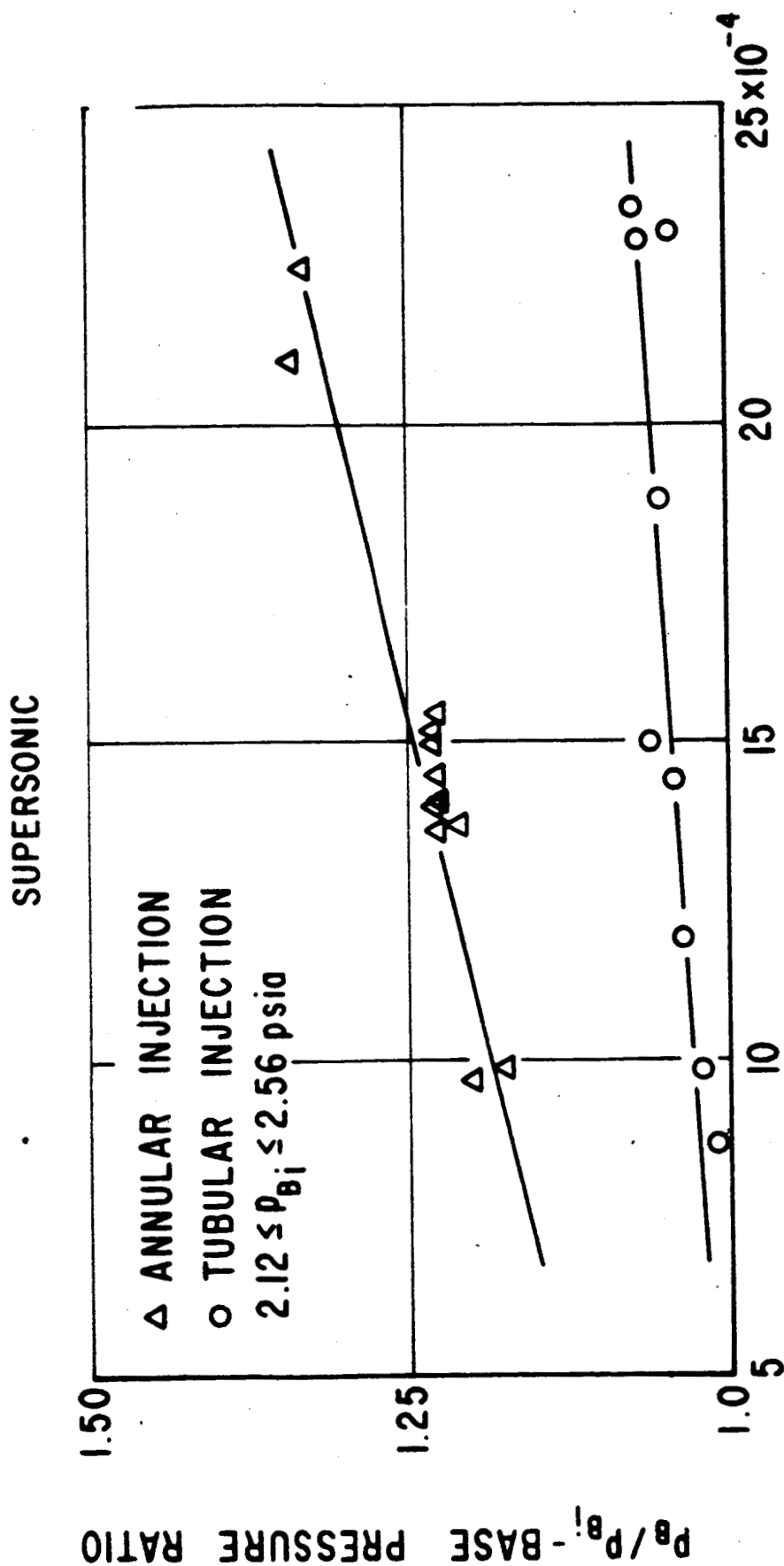


FIG. II RESULTS OF CONCENTRATION MEASUREMENT - SUBSONIC





\dot{m}_{H_2}/\dot{m}_T - FUEL TO TUNNEL FLOW RATIO

FIG. 12 EFFECT OF INJECTION ON BASE PRESSURE (NO COMBUSTION)

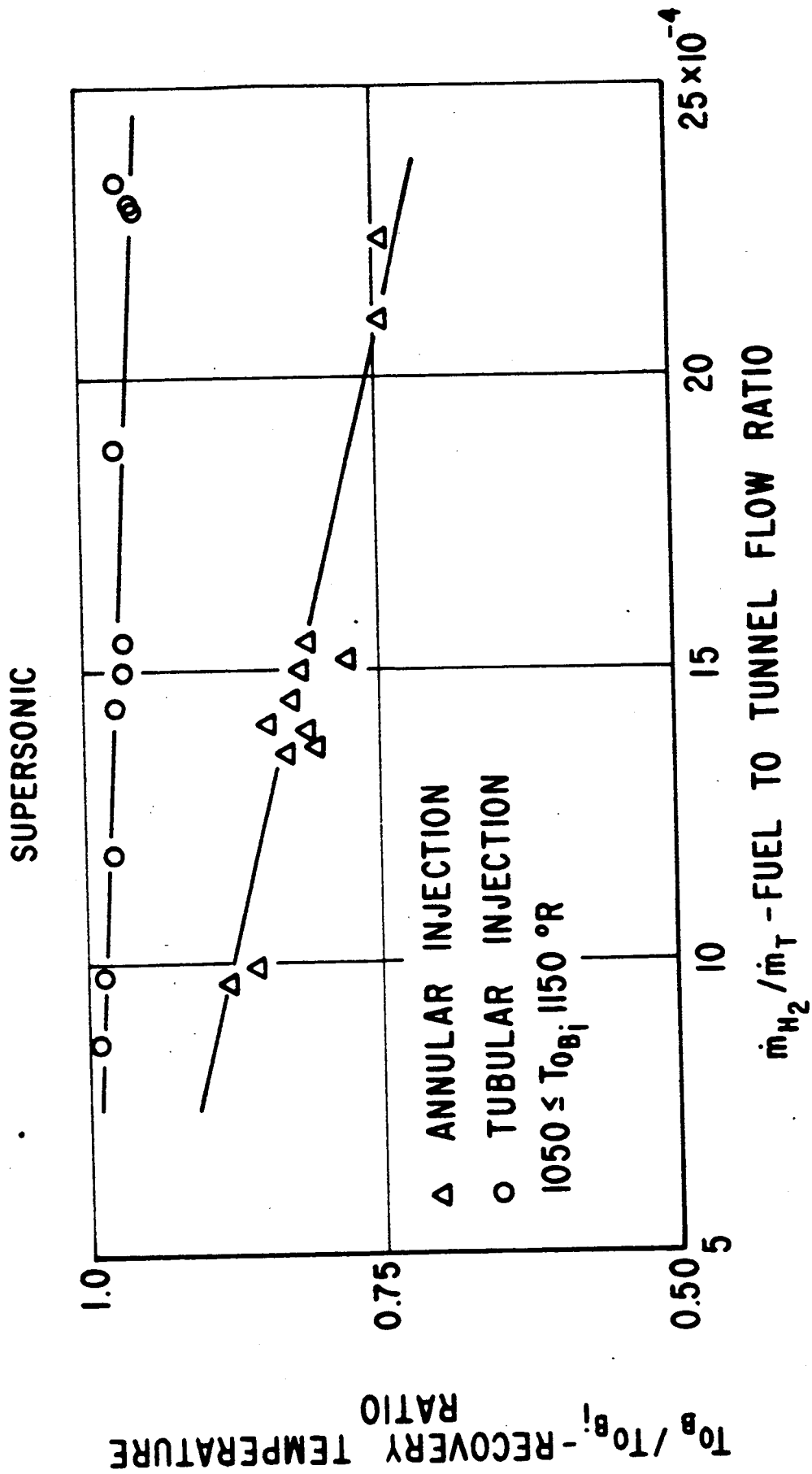


FIG 13 EFFECT OF INJECTION ON RECOVERY TEMPERATURE
(NO COMBUSTION)

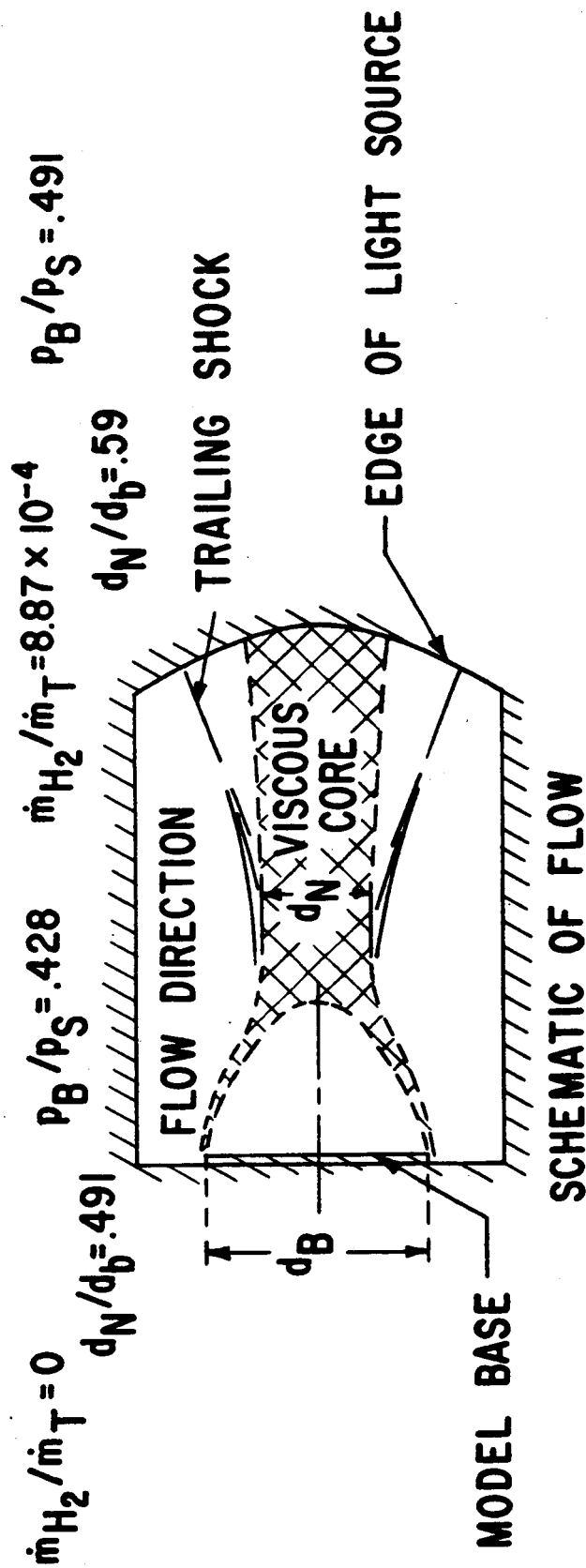
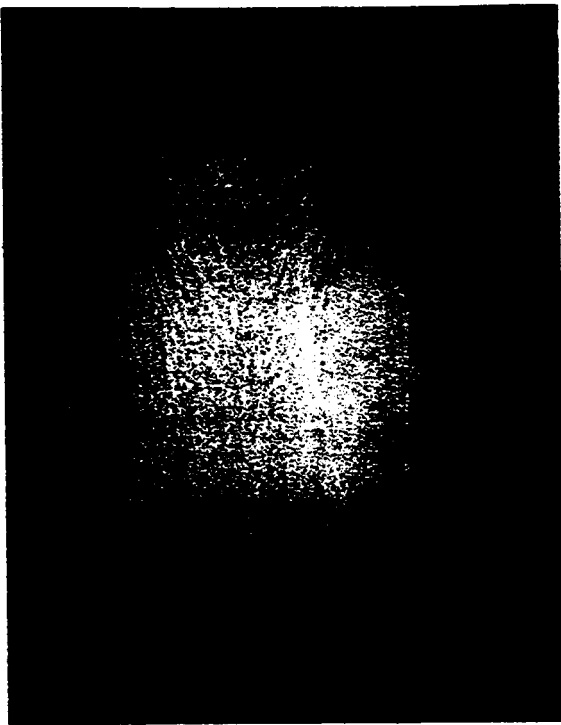
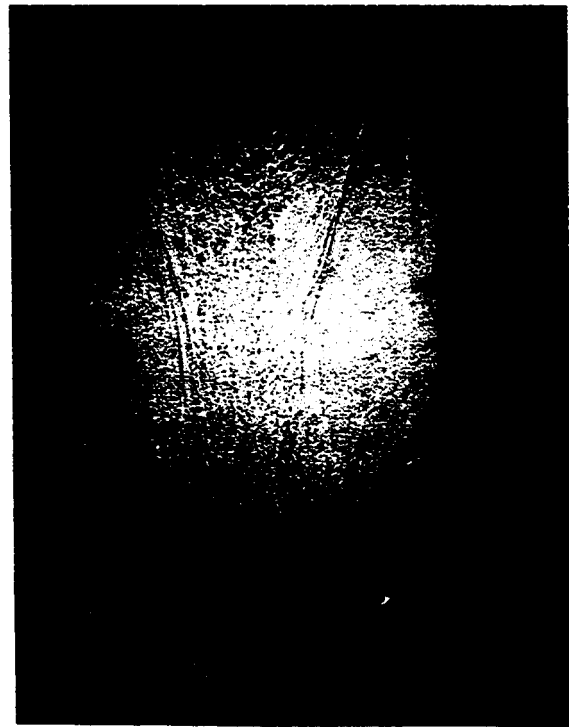


FIG. 14 - SHADOWGRAPH OF BASE FLOW REGION WITH AND WITHOUT INJECTION

○ TUBULAR INJECTION
△ ANNULAR INJECTION

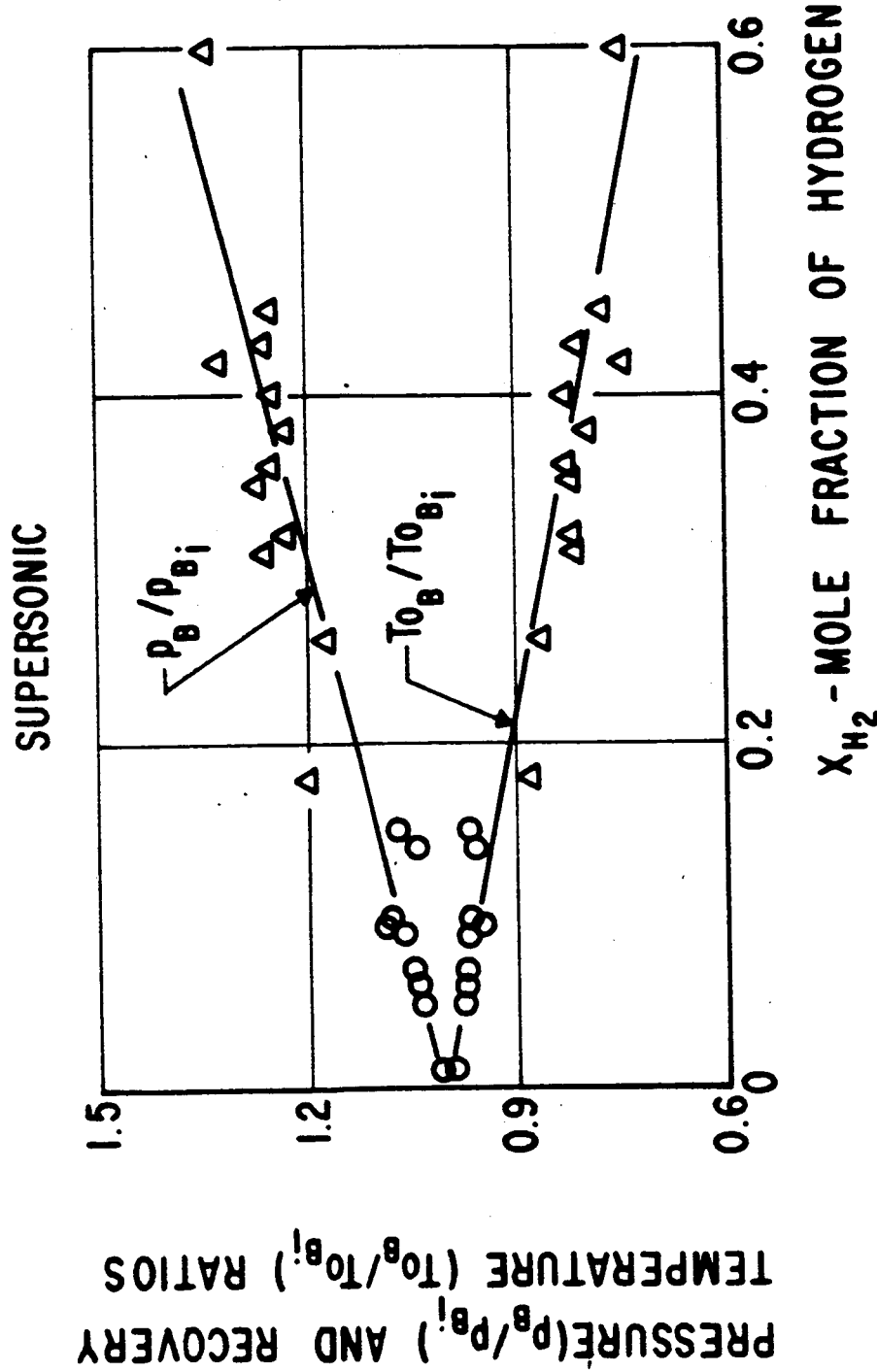


FIG. 15 CORRELATION OF EFFECTS OF INJECTION WITH CONCENTRATION IN THE RECIRCULATION ZONE (NO COMBUSTION)



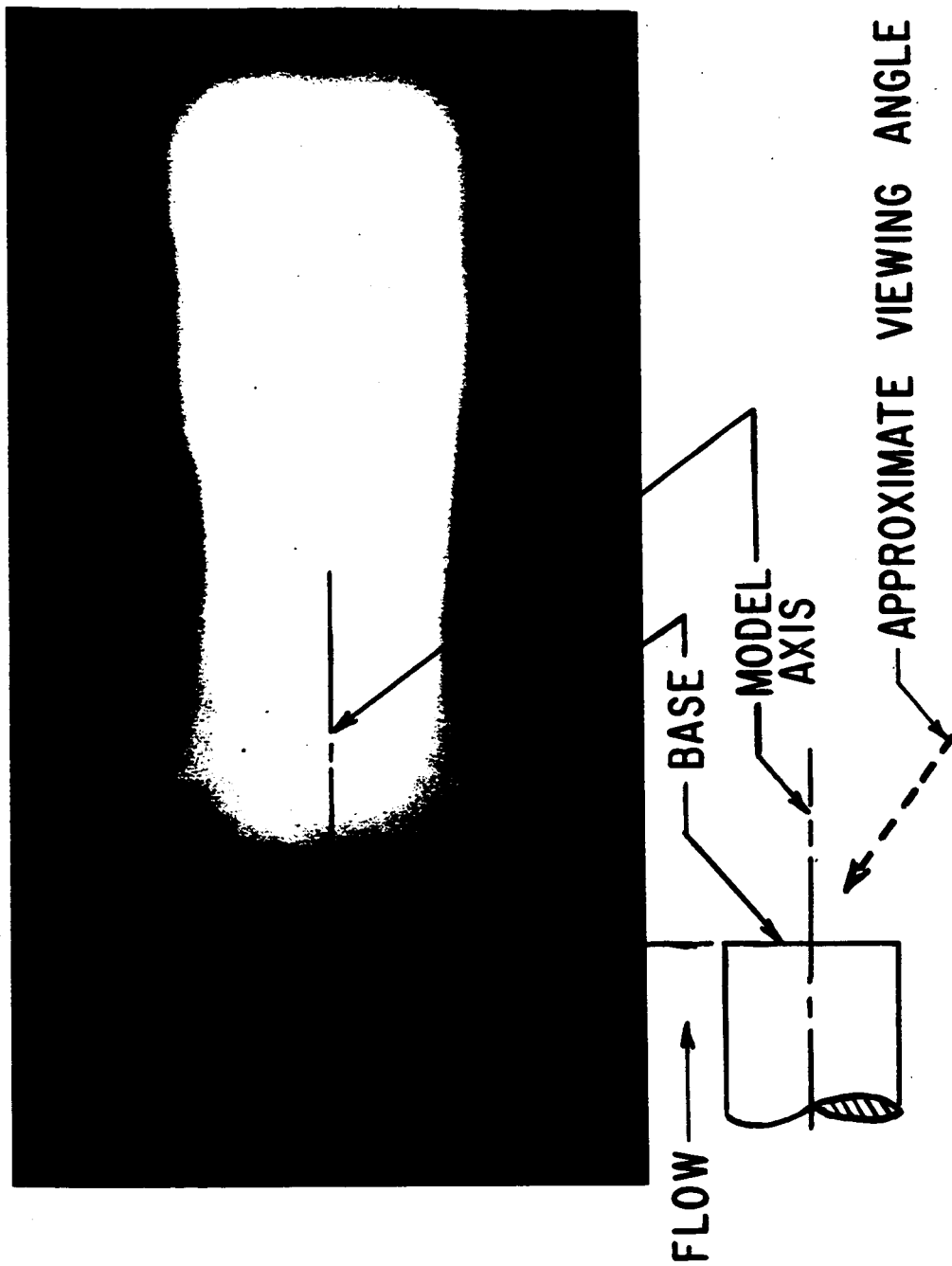


FIG.16 DIRECT PHOTOGRAPH OF BASE REGION WITH
COMBUSTION IN THE RECIRCULATION ZONE

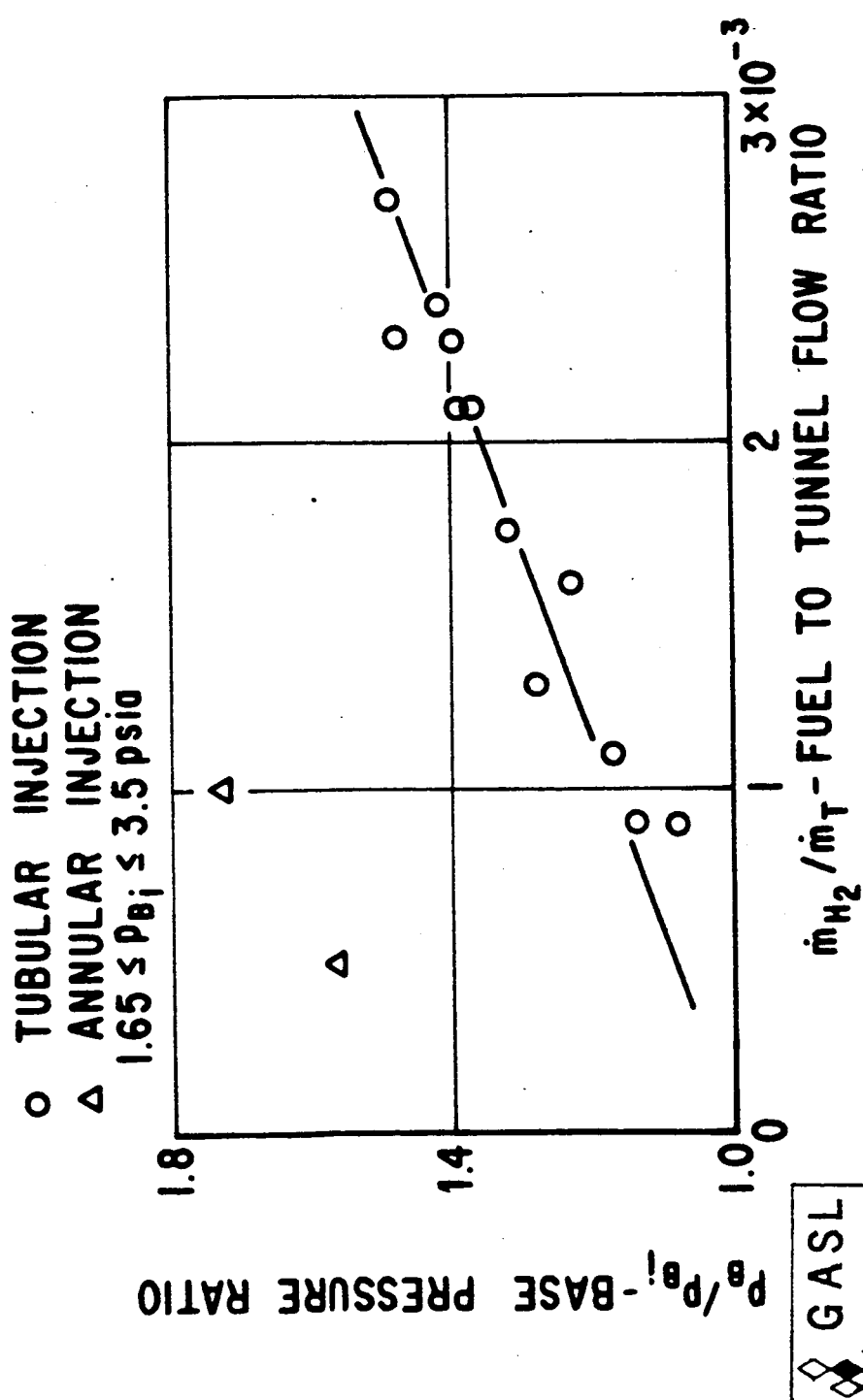
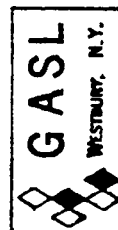


FIG. 17 EFFECT OF COMBUSTION ON BASE PRESSURE
(SUPERSONIC)



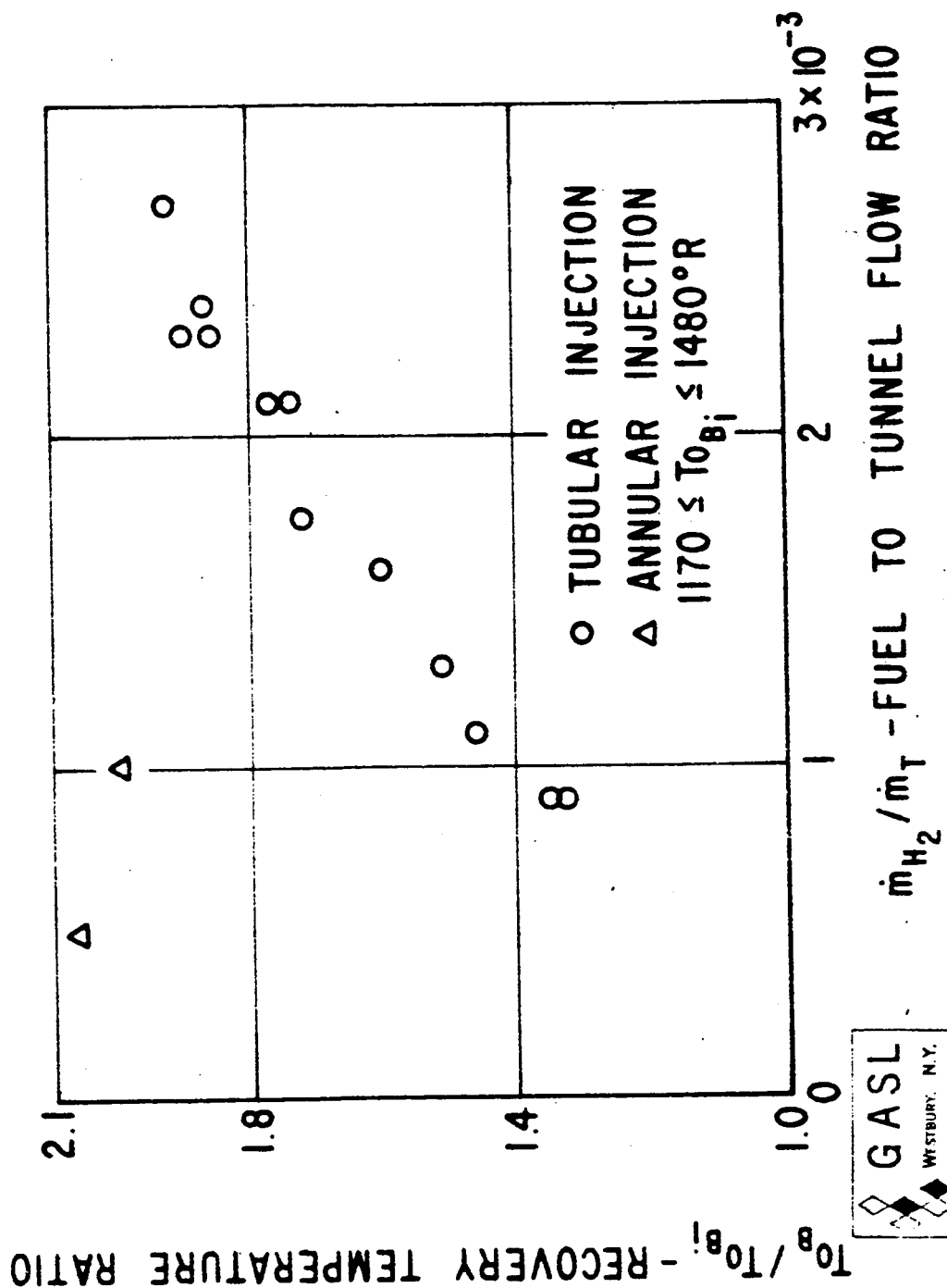


FIG. 18 EFFECT OF COMBUSTION ON RECOVERY TEMPERATURE
(SUPERSONIC)

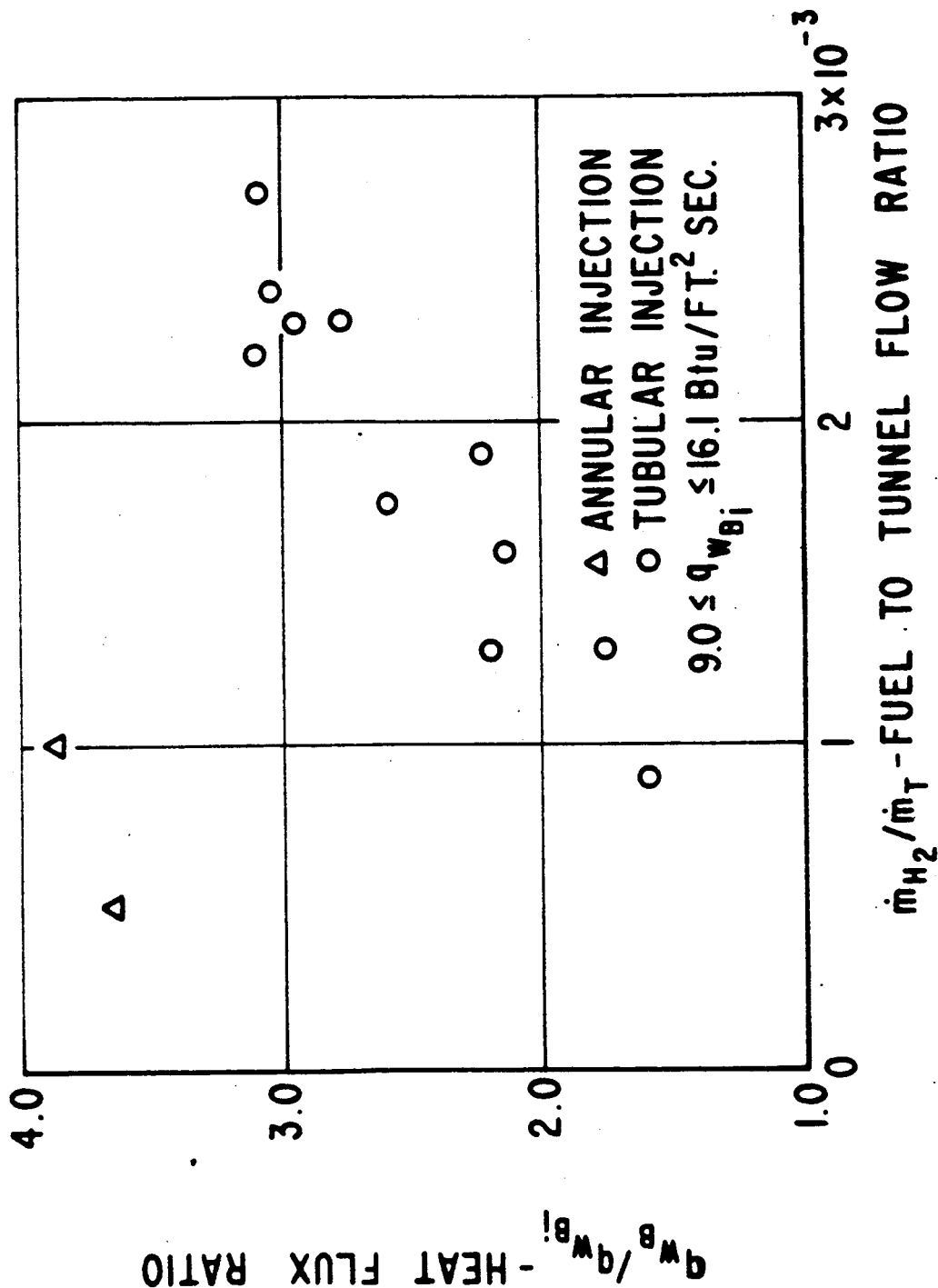
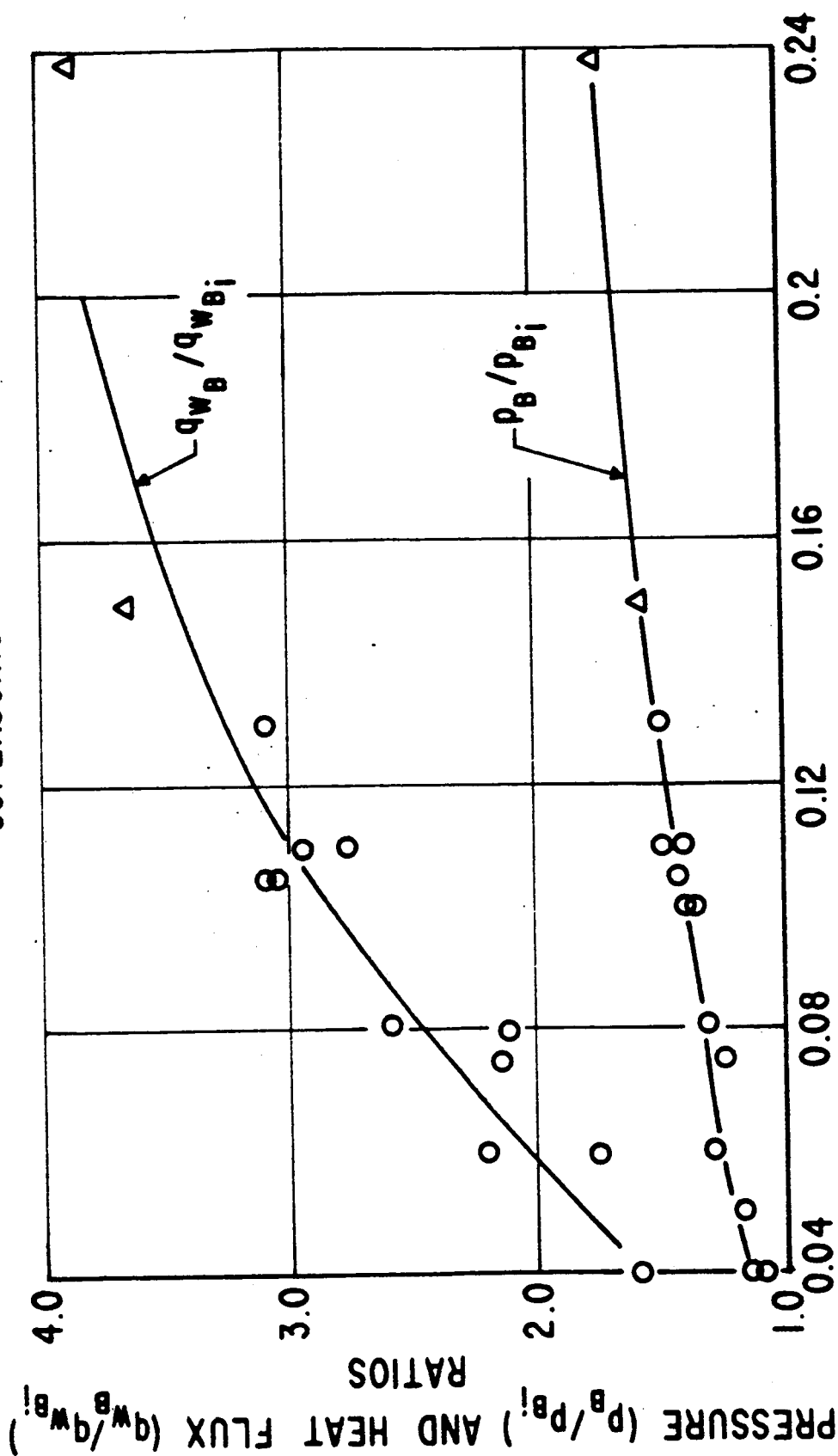


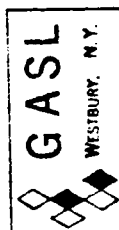
FIG. 19 EFFECT OF COMBUSTION ON BASE HEAT TRANSFER
(SUPERSONIC)

SUPERSONIC



\bar{X}_{H_2} - ESTIMATED MOLE FRACTION

FIG. 20 CORRELATION OF BASE PRESSURE AND HEAT TRANSFER WITH CONCENTRATION IN THE RECIRCULATION ZONE (COMBUSTION)



SUPERSONIC

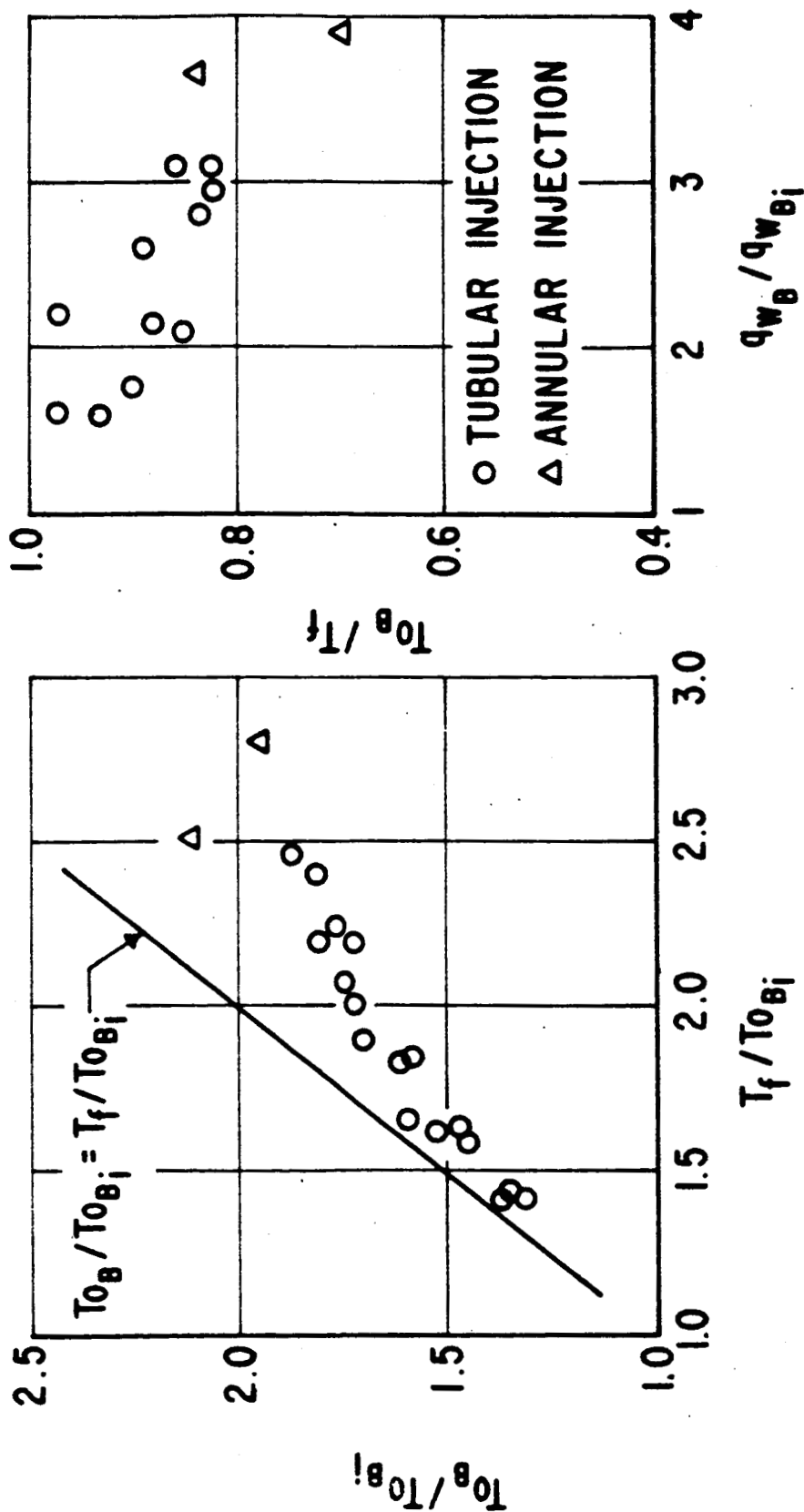


FIG. 21 COMPARISON OF MEASURED RECOVERY TEMPERATURE WITH ADIABATIC TEMPERATURE T_f

FIG. 22 EFFECT OF BASE HEATING ON RECOVERY TEMPERATURE

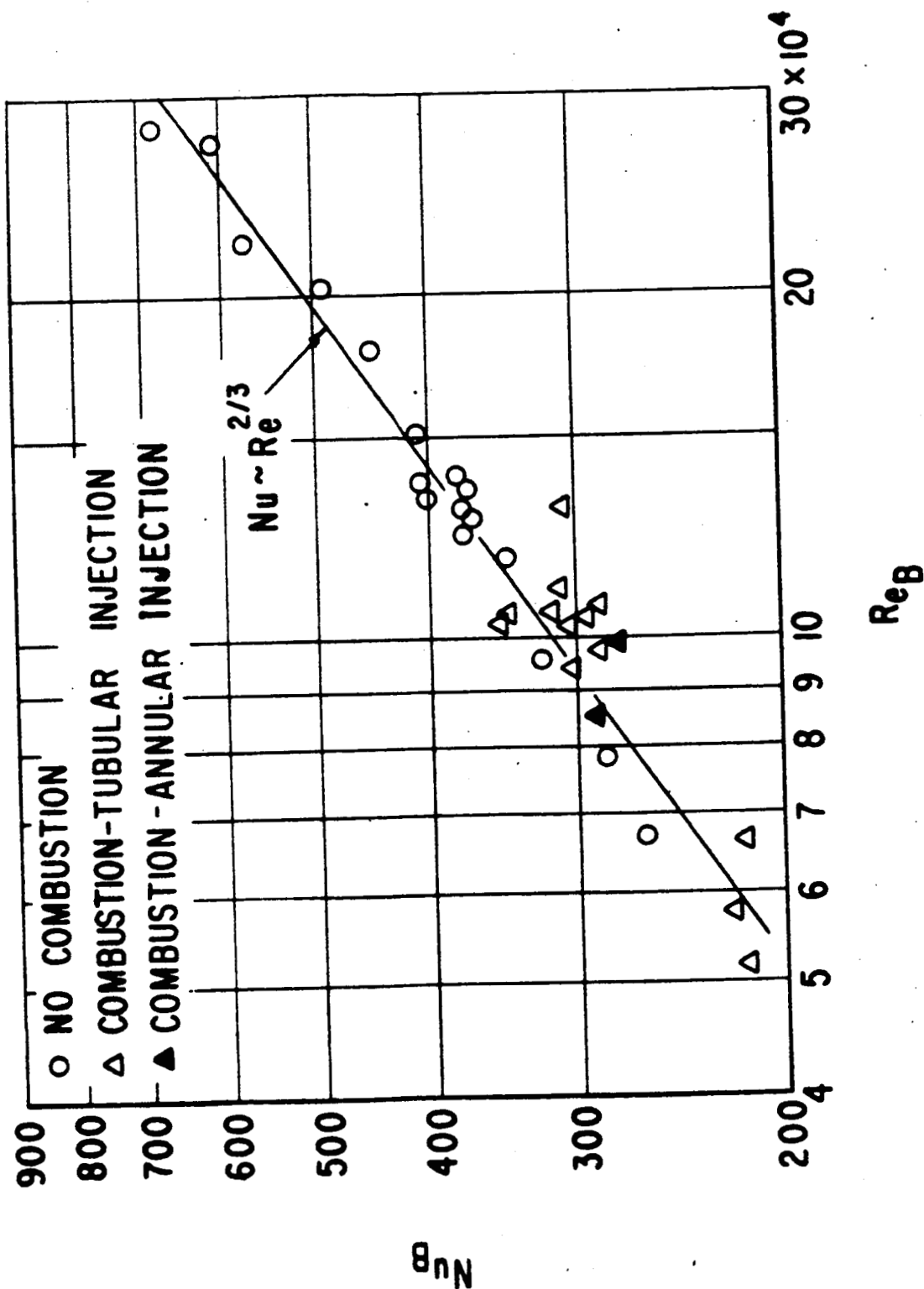


FIG. 23 BASE HEAT TRANSFER RESULTS WITH AND WITHOUT COMBUSTION - SUPERSONIC

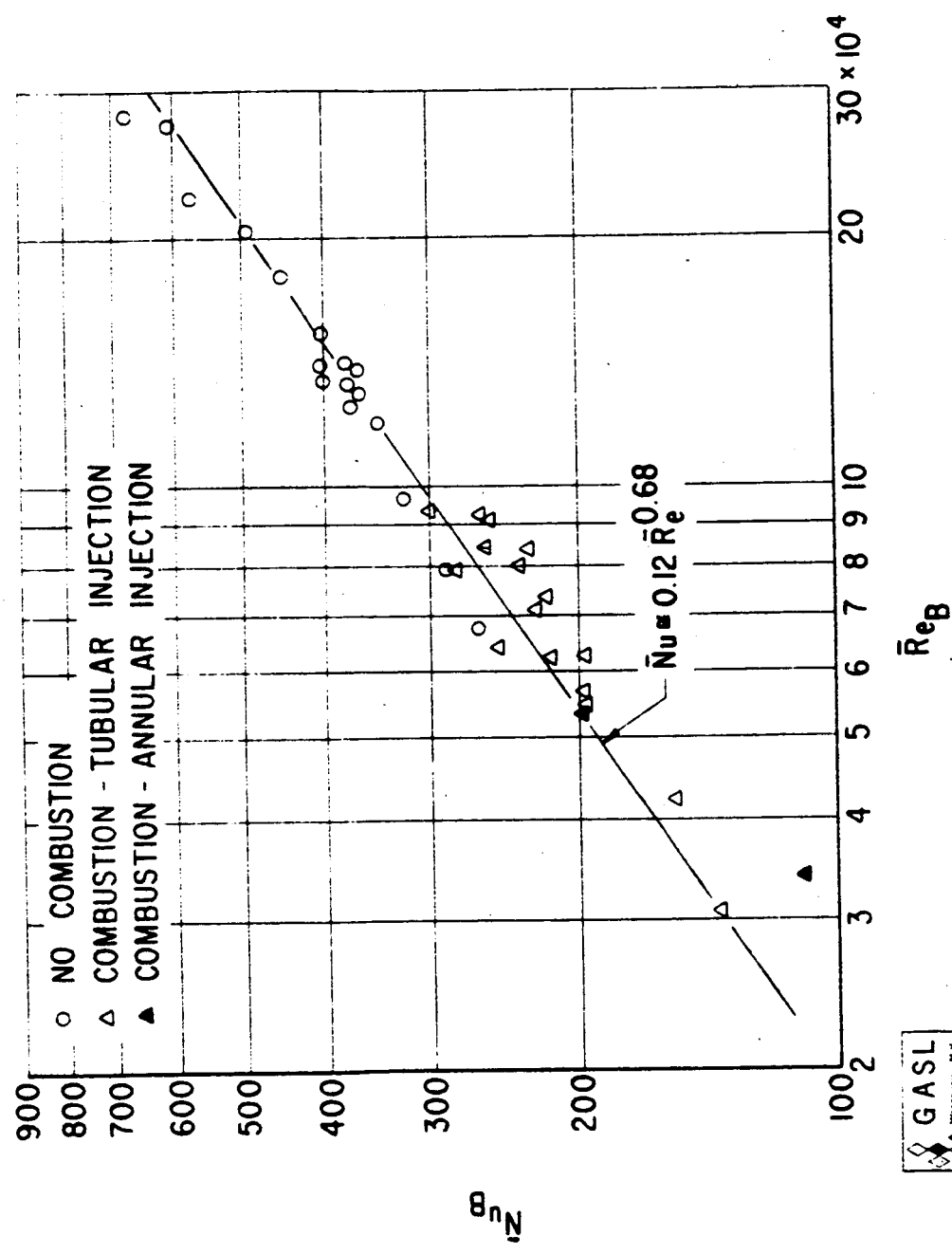


FIG. 24 CORRELATION OF BASE HEAT TRANSFER RESULTS - SUPERSONIC



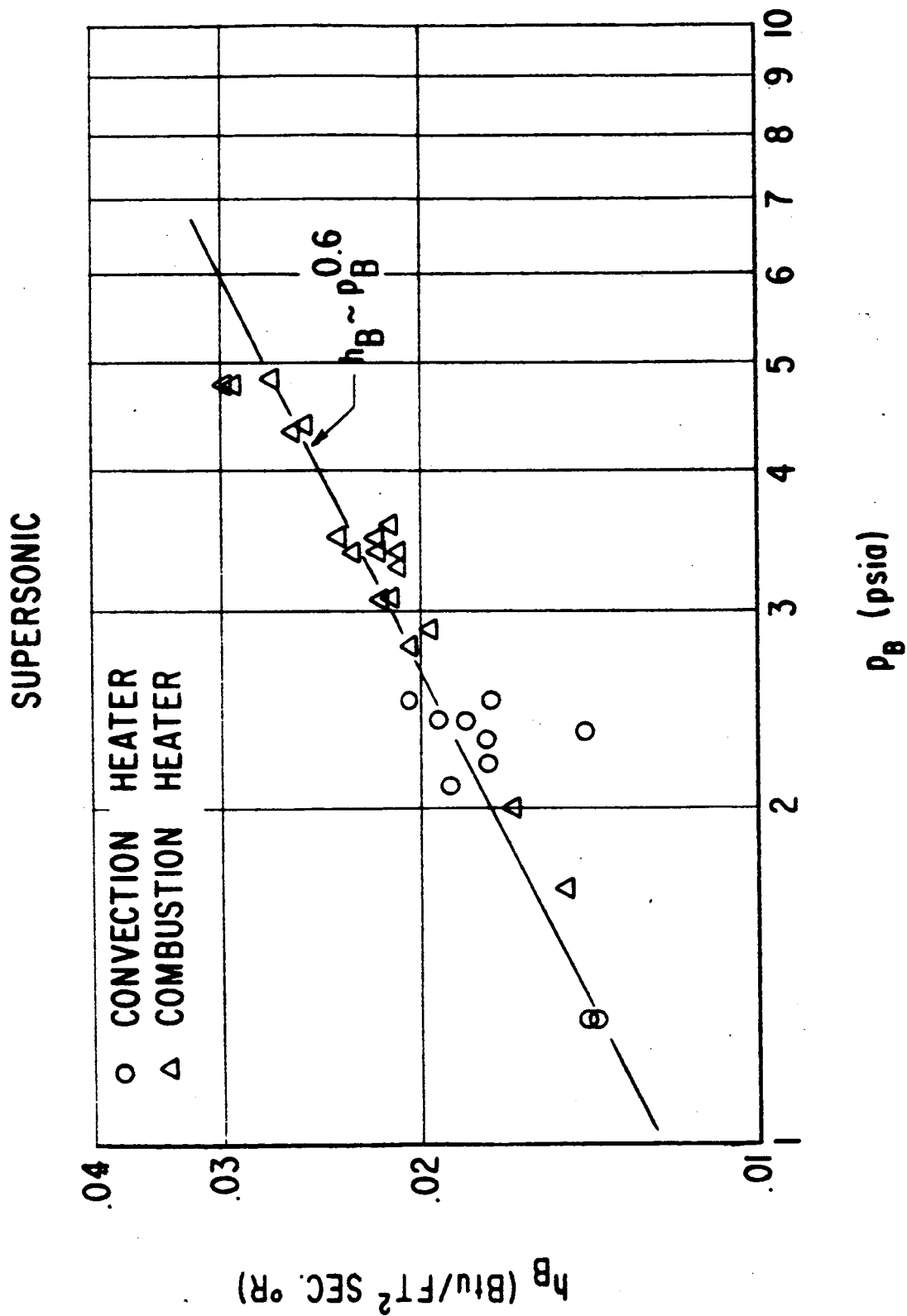


FIG. 25 VARIATION OF HEAT TRANSFER COEFFICIENT WITH BASE PRESSURE (NO INJECTION)

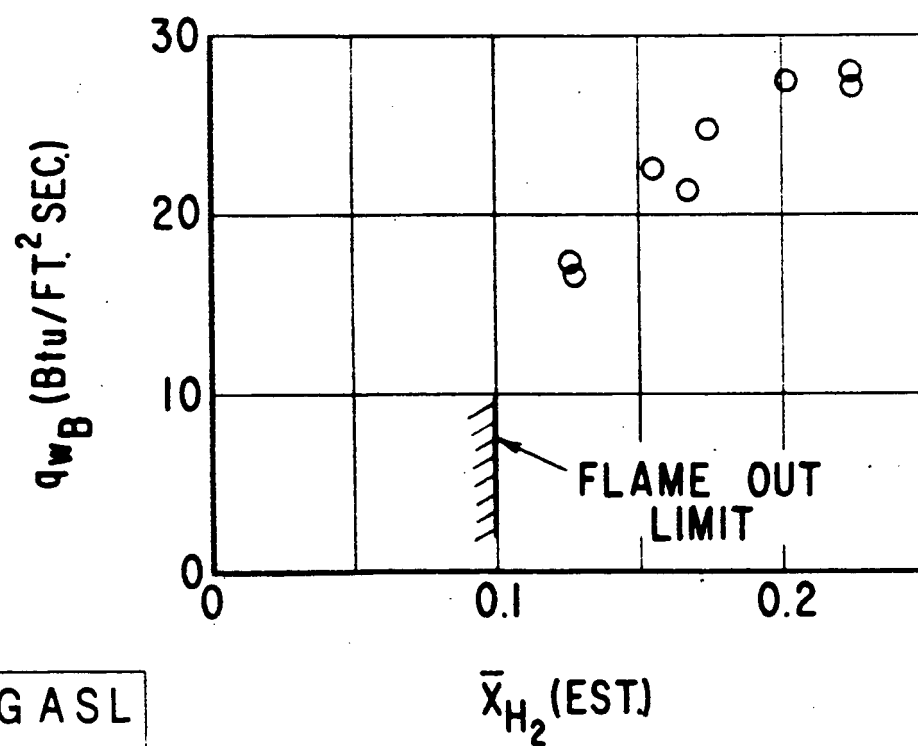
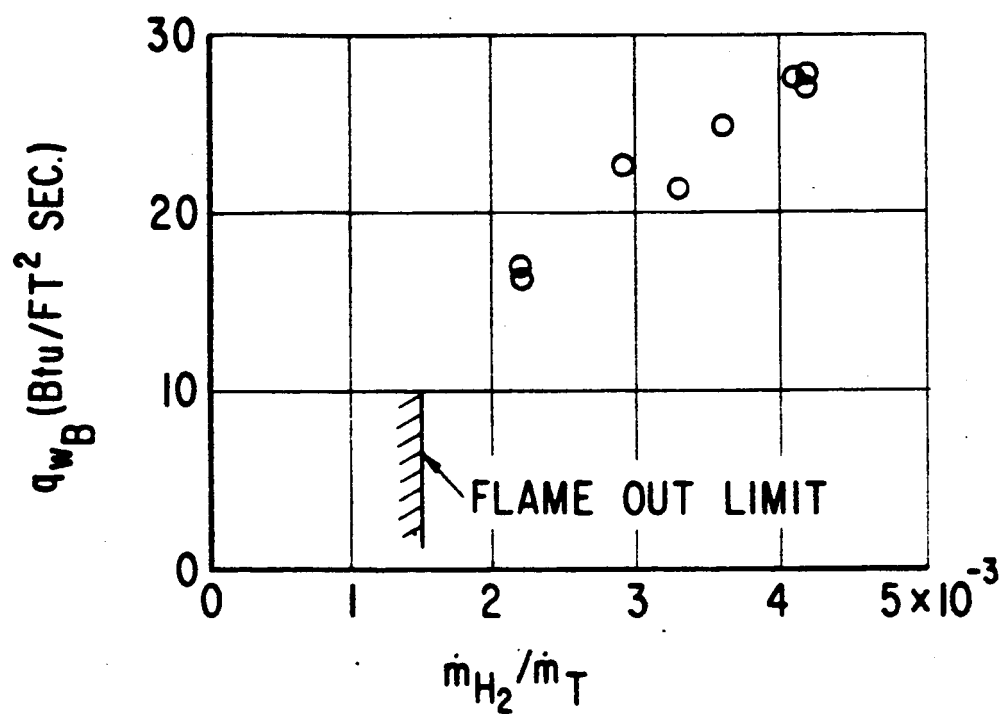
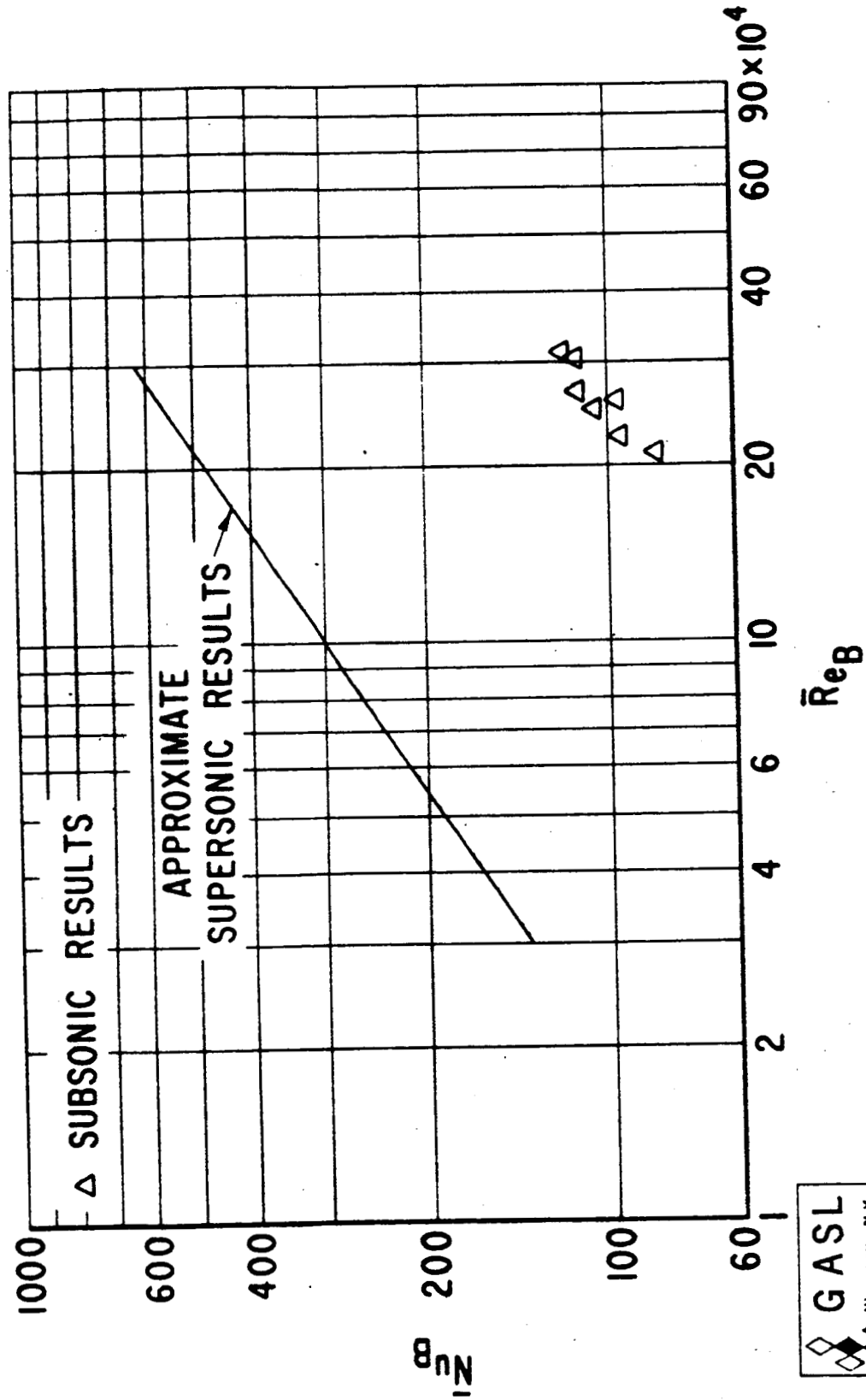


FIG. 26 SUBSONIC HEAT TRANSFER RESULTS



GASL
WESTBURY, N. Y.

FIG. 27 COMPARISON OF SUPERSONIC AND SUBSONIC RESULTS FOR
BASE HEAT TRANSFER

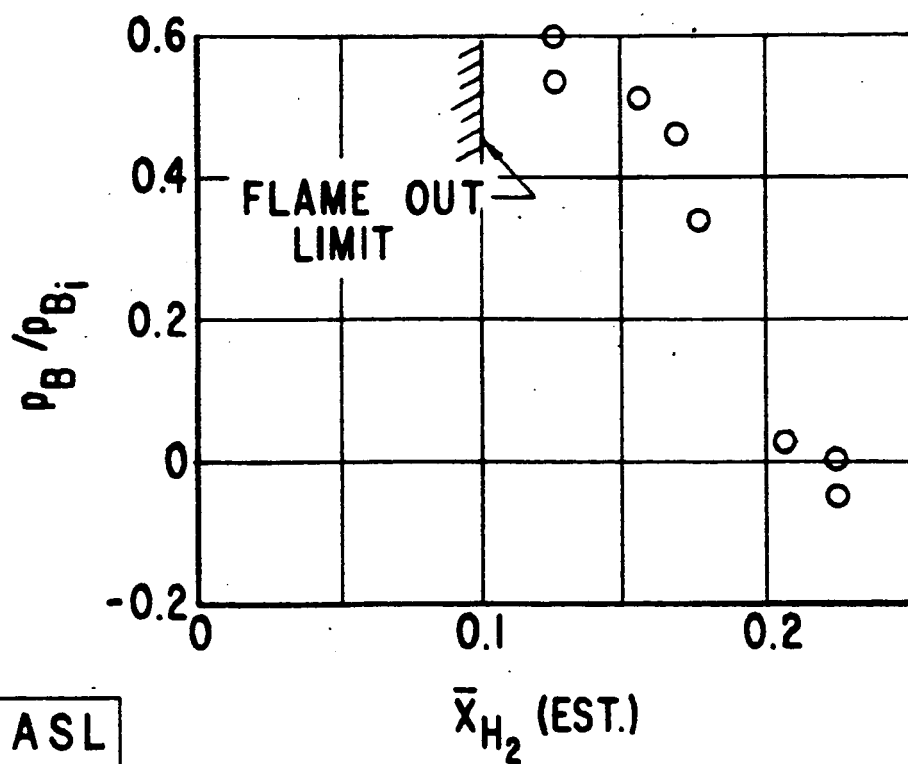
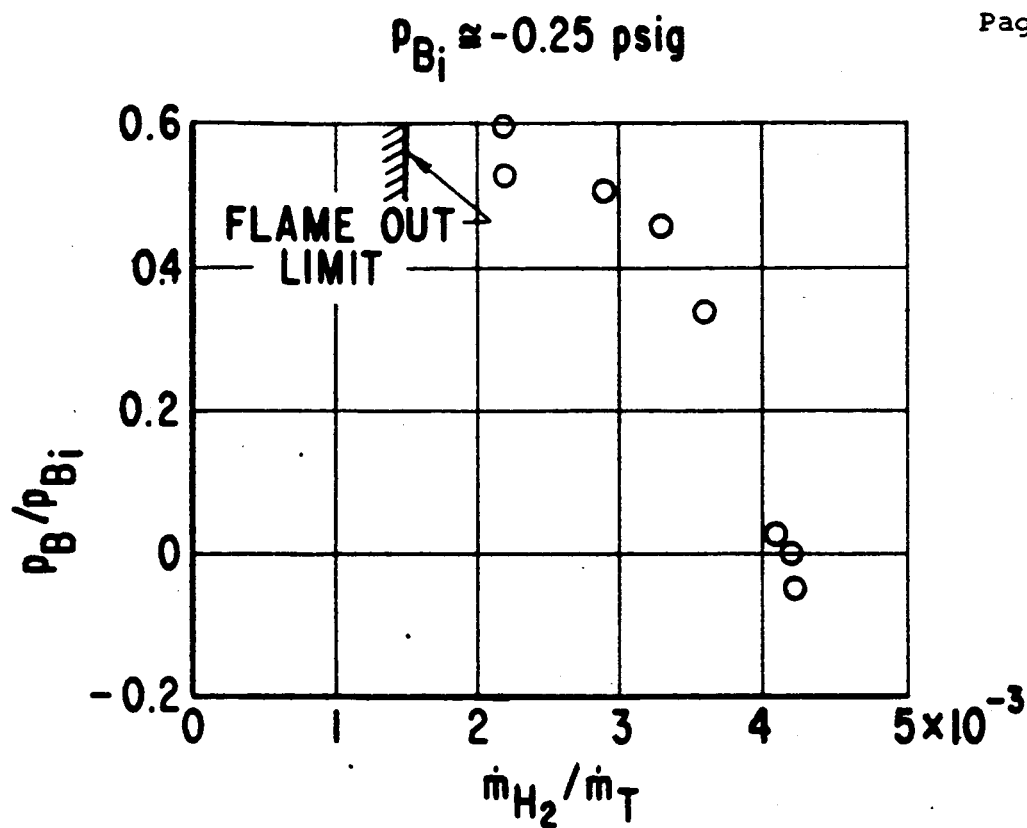


FIG. 28 EFFECT OF COMBUSTION ON BASE PRESSURE
(SUBSONIC)